Characterization of Electrically Small Radiating Sources by Tests Inside a Transmission Line Cell

Ippalapalli Sreenivasia [1]

David C. Chang [1]

Mark T. Ma [2]

[1] University of Colorado
Boulder, Colorado 80309

[2] Electromagnetic Fields Division
National Engineering Laboratory
National Bureau of Standards
Boulder, Colorado 80303

U.S. DEPARTMENT OF COMMERCE, Philip M. Klutznick, Secretary
Luther H. Hodges, Jr., Deputy Secretary
Jordan J. Baruch, Assistant Secretary for Science and Technology

NATIONAL BUREAU OF STANDARDS, Ernest Ambler, Director

Issued February 1980

NATIONAL BUREAU OF STANDARDS TECHNICAL NOTE 1017

Nat. Bur. Stand. (U.S.), Tech. Note 1017, 68 pages (Feb. 1980)
CODEN: NBTNAE

U.S. GOVERNMENT PRINTING OFFICE
WASHINGTON: 1980

For sale by the Superintendent of Documents, U.S. Government Printing Office, Washington, D.C. 20402

Stock No. 003-003-02157-1 Price $3.50 (Add 25 percent additional for other than U.S. mailing)

FOREWORD

This report describes theoretical and experimental analyses developed by staff of the University of Colorado at Boulder in collaboration with the Electromagnetic Fields Division of the National Bureau of Standards (NBS), under a contract sponsored by NBS. Professor David C. Chang heads the University team. Mark T. Ma of NBS serves as the technical contract monitor. The period covered by this report extends from August 1978 to June 1979.

The work described in this report represents a further aspect of technical analyses of transverse electromagnetic (TEM) transmission line cells developed at NBS. The purpose of this effort is to evaluate the use of TEM cells for (1) measuring the total rf radiated power by a device inserted into the cell for test, or (2) performing necessary susceptibility tests on a small electronic device.

Starting with the premise that an electrically small radiating object of arbitrary nature can be characterized by a composite dipole system consisting of three orthogonal electric and three orthogonal magnetic dipoles excited with arbitrary amplitudes and phases, this report presents measurement procedures and analytical derivations for determining the total emission and free-space radiation pattern of the radiating source. The relevant theoretical analysis is given first, followed by a general measurement procedure. The ensuing simplifications for determining just the total power radiated by the equipment under test (EUT) are then discussed. When the EUT is characterized by only electric or magnetic dipoles, the measurement procedure is extended to cells that do not support the TEM mode. The needed modifications in the measurement procedure, when the transition regions of the cell are mismatched, are also discussed.

The measurement procedure described in this report is simple to carry out once the normalized field distribution corresponding to the fundamental mode in the cell is determined. This can be

achieved from a known theoretical expression or by measurements with a probe. Experimental results for some selected cases are found in good agreement with the theoretical prediction.

Previous publications under the same effort include:

Tippett, J. C., and Chang, D. C., Radiation characteristics of dipole sources located inside a rectangular coaxial transmission line, NBSIR 75-829 (Jan. 1976).

Tippett, J. C., Chang, D. C., and Crawford, M. L., An analytical and experimental determination of the cut-off frequencies of higher-order TE modes in a TEM cell, NBSIR 76-841 (June 1976).

Tippett, J. C., and Chang, D. C., Higher-order modes in rectangular coaxial line with infinitely thin inner conductor, NBSIR 78-873 (March 1978).

Sreenivasiah, I., and Chang, D. C., A variational expression for the scattering matrix of a coaxial line step discontinuity and its application to an over moded coaxial TEM cell, NBSIR 79-1606 (May 1979).

Tippett, J. C., and Chang, D. C., Dispersion and attenuation characteristics of modes in a TEM cell with a lossy dielectric slab, NBSIR 79-1615 (Aug. 1979).

TABLE OF CONTENTS

LIST OF ILLUSTRATIONS AND TABLES

CHARACTERIZATION OF ELECTRICALLY SMALL RADIATING SOURCES BY TESTS INSIDE A TRANSMISSION LINE CELL

Ippalapalli Sreenivasiah
David C. Chang
and
Mark T. Ma

An electrically small radiating source of arbitrary nature may be modeled by an equivalent dipole system consisting of three orthogonal electric dipoles and three orthogonal magnetic dipoles, each excited with arbitrary phase. An experimental procedure for determining the emission characteristics of such an equivalent dipole system by tests inside a single-mode transmission line cell is described in this report, followed by some experimental results.

1. INTRODUCTION

Currently there is a considerable interest in developing methods for measuring electromagnetic (EM) emissions and EM susceptibility of electronic equipment [1]. Rectangular coaxial transverse electromagnetic (TEM) cells (fig. 1) developed at the National Bureau of Standards (NBS) [2-5] for this purpose are quite satisfactory for establishing a standard test field environment for such measurements. However, one must devise a method to relate measurements taken inside the cell to the free-space radiation characteristics of the object. In this report, we consider a typical equipment under test (EUT) as consisting of an electrically small box housing low-frequency ac circuits. Leakage currents to the exterior surface may be replaced by equivalent electric/magnetic dipoles with appropriate magnitudes and phases, and all such dipoles may be combined to form a composite source consisting of three orthogonal electric and three orthogonal magnetic dipoles with appropriate moments and excitation phases. The question then is to determine the unknown moments and phases of the individual electric and/or magnetic dipoles of which the composite source, characterizing the EUT, is made. Total radiation power of the EUT and its far-field characteristics in free-space are then determined from values of

these composite dipoles. In section 2 we give theoretical expressions for the modal amplitudes of the fields radiated, in the positive and negative directions of a uniform cylindrical guide, by arbitrary dipole sources located inside the guide.

For a symmetrical cell, separation of the electric and magnetic dipole sources is achieved by taking the sum and difference of outputs from the two ends of the TEM waveguide enclosing the sources. A measurement procedure, which enables one to obtain the needed parameters for determining the free-space radiation pattern of and the total power radiated by a composite source consisting of orthogonal electric and orthogonal magnetic dipoles, is then described in section 3.

In assessing the emission level of an EUT, we are often not interested in knowing the complete free-space radiation pattern but rather the free-space total radiated power. In such event, the measurement procedure is considerably simplified, as discussed in section 4, depending upon the geometry of the test cell and the type of the source.

Generally, a test cell consists of a section of uniform transmission line with matched transitions to 50-Ω coaxial connectors on both ends. In section 5 we discuss the effect of mismatched transitions and how to modify the measured results to account for such a mismatch. A procedure for determining the scattering matrices of the transitions is also described in the same section. Experimental results are given in section 6, followed by concluding remarks in section 7.

2. RADIATION CHARACTERISTICS OF DIPOLE SOURCES LOCATED INSIDE A TEM CELL

The electric and magnetic fields generated in the positive and negative z-directions by an electric and/or magnetic dipole in a guide of arbitrary cross section (fig. 2) may be represented in terms of individual modes inside the waveguide as

$$\bar{E}^{(\pm)} = \sum_n \binom{a}{b}_n \bar{E}_n^{(\pm)} \tag{2.1a}$$

$$\bar{H}^{(\pm)} = \sum_n \binom{a}{b}_n \bar{H}_n^{(\pm)} , \tag{2.1b}$$

where, with a time dependence of $e^{i\omega t}$,

$$\bar{E}_n^{(\pm)} = (\bar{e}_n \pm \bar{e}_{zn}) e^{\mp i\beta_n z} \tag{2.2a}$$

$$\bar{H}_n^{(\pm)} = (\pm\bar{h}_n + \bar{h}_{zn}) e^{\mp i\beta_n z} , \tag{2.2b}$$

$\bar{e}_n$, $\bar{h}_n$ are transverse vector functions, $\bar{e}_{zn}$ and $\bar{h}_{zn}$ are axial vector functions at any given cross section, and β_n is the propagation constant of the same mode. For E modes, $\bar{h}_{zn}$ is zero, while for H modes $\bar{e}_{zn}$ is zero. Orthogonality between two modes, each properly normalized, implies

$$\int_s \int \bar{e}_m \times \bar{h}_n \cdot \hat{z} ds = \delta_{mn} , \tag{2.3}$$

where s represents the cross-sectional area of the guide. Then, an application of the Lorentz reciprocity theorem, assuming that the waveguide walls are perfectly conducting, yields the amplitudes a_n, b_n of each mode in the positive and negative z-directions away from the dipole source [6]:

$$\binom{a}{b}_n = -\frac{1}{2} \int_C \bar{J} \cdot \bar{E}_n^{(\mp)} \, d\ell , \tag{2.4}$$

where the vector $\bar{J}$ represents the total current flowing through an infinitesimally thin current filament of a length described by C. For a short electric dipole, the above expression may be written as

$$\begin{pmatrix} a \\ b \end{pmatrix}_n = -\frac{1}{2}\,\bar{m}_e \cdot \bar{E}_n^{(\mp)} \,, \tag{2.5}$$

where $\bar{m}_e = \bar{J} d\ell$ is the strength of the dipole. If the current filament forms a closed loop of small cross section s, one obtains from eq (2.4)

$$\begin{pmatrix} a \\ b \end{pmatrix}_n = -\frac{1}{2}\,|\bar{J}| \int_C \bar{E}_n^{(\mp)} \cdot d\bar{\ell} = -\frac{1}{2}\,|\bar{J}| \int\int_s \nabla \times E_n^{(\mp)} \cdot \overline{ds}$$

$$= \frac{1}{2}\,(i\omega\mu_o)\,\bar{H}_n^{(\mp)} \cdot \bar{m}_m \,, \tag{2.6}$$

where $\bar{m}_m = |\bar{J}|\,\bar{s}$ is the magnetic dipole moment, ω is the angular frequency, and μ_o is the free-space permeability.

In general, both $\bar{m}_e$ and $\bar{m}_m$ are complex vector moments given by

$$\bar{m}_{\substack{e \\ m}} = \hat{x}\, m_{\substack{ex \\ mx}} e^{i\psi_{\substack{ex \\ mx}}} + \hat{y}\, m_{\substack{ey \\ my}} e^{i\psi_{\substack{ey \\ my}}} + \hat{z}\, m_{\substack{ez \\ mz}} e^{i\psi_{\substack{ez \\ mz}}} \,, \tag{2.7}$$

with $\hat{x}$, $\hat{y}$, and $\hat{z}$ representing unit vectors along the x-, y-, and

z-directions, respectively. Denoting the TEM mode by subscript o, we write

$$\bar{E}_o^{(\pm)} = (\hat{x}\, e_{ox} + \hat{y}\, e_{oy})\, e^{\mp ikz} , \qquad (2.8a)$$

$$\bar{H}_o^{(\pm)} = (\hat{x}\, h_{ox} + \hat{y}\, h_{oy})\, e^{\mp ikz} , \qquad (2.8b)$$

and note that

$$\bar{H}_o^{(\pm)} = \pm\, \hat{z} \times \bar{E}_o^{(\pm)} / \zeta_o , \qquad (2.9)$$

where k is the free-space wave number.

Using eqs (2.5) and (2.6), we may write the amplitudes of the radiated fields corresponding to a combined presence of electric and magnetic dipoles as

$$\binom{a}{b} = -\frac{1}{2}\left[\bar{m}_e \cdot \bar{e}_o \pm i\, k\, \bar{m}_m \cdot (\hat{z} \times \bar{e}_o)\right]$$

$$= -\frac{1}{2}\left(\bar{m}_e \pm i\, k\, \bar{M}\right) \cdot \bar{e}_o \qquad (2.10a)$$

where

$$\bar{M} = \bar{m}_m \times \hat{z} \; ; \quad \bar{e}_o = (e_{ox}\, \hat{x} + e_{oy}\, \hat{y}) \qquad (2.10b)$$

so that

$$a^{*} + b = - \bar{m}_e \cdot \bar{e}_o \qquad (2.11a)$$

$$a - b = - i k (\bar{m}_m \times \hat{z}) \cdot \bar{e}_o \quad . \qquad (2.11b)$$

In obtaining eq (2.10a) we have assumed that only the dominant TEM mode exists inside the cell. The subscript o has been omitted to simplify the notation. The relations in eqs (2.11a) and (2.11b) derived above are very important in determining the strengths of dipole sources (electric and/or magnetic) located inside a TEM transmisison line. This will be clearer if we consider the experimental setup shown in figure 3 where the test object is placed at a point $(x_o, y_o, 0)$ with respect to a frame of reference, in x-, y-, and z-coordinates, which is fixed with respect to the cell. The outputs from the two ends of the cell are added in phase or out of phase with each other by means of a 180° phase shifter. In practice, one may obtain the sum/difference at one port by short circuiting the other port at distance of an odd/even number of quarter wavelengths away from the test object (assuming that the end transitions are perfectly matched). We note that the sum power $P_s = (a+b)(a+b)^*$ is independent of the magnetic dipole while the difference power $P_d = (a-b)(a-b)^*$ is independent of the electric dipole. Furthermore, only the components of $\bar{m}_e$ and $\bar{M}$ that are along the direction of the transverse electric field vector $\bar{e}_o(x_o, y_o, 0)$ contribute to the output. In the following sections, we describe some experimental procedures, which are based on the preceding observations, for determining the radiation characteristics of electric and/or magnetic dipole sources by placing them inside a single-mode TEM cell.

3. DETERMINATION OF RADIATION CHARACTERISTICS OF DIPOLE SOURCES BY TESTS INSIDE A TEM CELL

In this section we describe the experimental procedure for tests taken inside a cell consisting of a section of TEM transmission line, with perfectly conducting inner and outer conductors, and perfectly matched transitions at both ends. As shown in Appendix I, the free-space radiation chracteristics of an EUT characterized by three orthogonal electric or magnetic dipoles can be completely determined through the quantities

$$m_{\underset{m}{ex}}^2,\ m_{\underset{m}{ey}}^2,\ m_{\underset{m}{ez}}^2,\ m_{\underset{m}{ex}}\, m_{\underset{m}{ey}} \cos(\psi_{\underset{m}{ex}} - \psi_{\underset{m}{ey}}),\ m_{\underset{m}{ey}}\, m_{\underset{m}{ez}} \cos(\psi_{\underset{m}{ey}} - \psi_{\underset{m}{ez}}),$$

and $m_{\underset{m}{ez}}\, m_{\underset{m}{ex}} \cos(\psi_{\underset{m}{ez}} - \psi_{\underset{m}{ex}})$.

3.1 Measurement Procedure

To obtain the twelve unknown quantities mentioned above, we first establish two frames of reference (x,y,z) and (x',y',z'), the former fixed with respect to the cell with the origin (0) at the geometric center of the cell and the latter fixed with respect to the EUT with the origin (0') at the center of the EUT. As shown in figure 3, let the z-axis be along the length of the cell, the y-axis be perpendicular to the center septum, and the x-axis be along the width of the septum. Then we go through the following sequence of measurement operations where all the rotations are assumed to be in the counter-clockwise direction.

(1) Position the EUT at a convenient test point $(x_o, y_o, 0)$ such that its x'-, y'-, and z'-axes (designated initially as $\bar{x}$-, $\bar{y}$-, and $\bar{z}$-axes in figure 3) are along the directions of x-, y-, and z-axes, respectively.

(2) Rotate the EUT about its z'-axis by an angle of θ_o in

the counter-clockwise direction, θ_o being a convenient value ranging from 0 to $\pi/2$. This angle θ_o and the test point $(x_o, y_o, 0)$ shall remain fixed throughout the experiment. Measure the sum power P_{s1} and the difference power P_{d1} for this orientation (fig. 4a) of the EUT. The sum power is obtained by removing the 180° phase shifter (fig. 3) from the circuit, and the difference power is obtained by placing the phase shifter in the circuit.

(3) Rotate the EUT by 90° about its z'-axis from the position in step (2). Measure the sum power P_{s2} and the difference power P_{d2}.

(4) Position the EUT at the test point such that x'-, y'-, and z'-axes are along z-, x-, and y-axes, respectively. Rotate the EUT by an angle θ_o about its x'-axis and measure the sum power P_{s3} and the difference power P_{d3} corresponding to this orientation (fig. 4b).

(5) Rotate the EUT by 90° about the x'-axis from its position in step (4) and measure the sum and difference powers P_{s4} and P_{d4}.

(6) Position the EUT at the test point such that x'-, y'-, and z'-axes are along y-, z-, and x-axes, respectively. Rotate EUT by an angle θ_o about its y'-axis and measure the powers P_{s5} and P_{d5} corresponding to this orientation (fig. 4c).

(7) Rotate the EUT by 90° about the y'-axis from its position in step (6) and measure the sum and difference powers P_{s6} and P_{d6}.

3.2 Interpretation of the Results

Noting that in eqs (2.11a) and (2.11b)

$$\underset{m}{m_{ex}},\ \underset{m}{m_{ey}},\ \underset{m}{m_{ez}}$$

represent the respective components of the dipole moments along x-, y-, and z-axes of the TEM cell, we obtain the following matrix equations for the unknown moments

$$m'_{ex}, \; m'_{ey}, \; m'_{ez}$$

along the x'-, y'-, and z'-axes of the EUT and the cross components:

$$\overline{B}\,\overline{M}_e = \overline{P}_s \tag{3.1a}$$

$$\overline{B}\,\overline{M}_m = \overline{P}_d/(k^2) \; , \tag{3.1b}$$

where

$$\overline{B} = \begin{pmatrix} p'^2 & q'^2 & 0 & 2p'q' & 0 & 0 \\ q'^2 & p'^2 & 0 & -2p'q' & 0 & 0 \\ 0 & p'^2 & q'^2 & 0 & 2p'q' & 0 \\ 0 & q'^2 & p'^2 & 0 & -2p'q' & 0 \\ q'^2 & 0 & p'^2 & 0 & 0 & 2p'q' \\ p'^2 & 0 & q'^2 & 0 & 0 & -2p'q' \end{pmatrix} \tag{3.1c}$$

$$\overline{M}_e = [m'^2_{ex} \quad m'^2_{ey} \quad m'^2_{ez} \quad m'_{exy} \quad m'_{eyz} \quad m'_{ezx}]^T \tag{3.1d}$$

$$\bar{P}_s = [\, P_{s1}\ P_{s2}\ P_{s3}\ P_{s4}\ P_{s5}\ P_{s6}]^T \tag{3.1e}$$

$$\bar{P}_d = [P_{d2}\ P_{d1}\ P_{d4}\ P_{d3}\ P_{d6}\ P_{d5}]^T \tag{3.1f}$$

$$p' = p \cos \theta_o + q \sin \theta_o \tag{3.1g}$$

$$q' = q \cos \theta_o - p \sin \theta_o \tag{3.1h}$$

$$p = \bar{e}_o\ (x_o, y_o) \cdot \hat{x} \tag{3.1i}$$

$$q = \bar{e}_o\ (x_o, y_o) \cdot \hat{y}\ , \tag{3.1j}$$

and we use the notation

$$m'_{exy} = m'_{ex}\ m'_{ey}\ \cos(\psi_{ex} - \psi_{ey})\ , \text{ etc.}$$

The solution to the previous equations is readily given by

$$[\, m'^{2}_{ex} \; m'^{2}_{ey} \; m'^{2}_{ez} \,]^{T} = \frac{1}{2} \bar{C} \, \bar{P}_s \, / \, | \, \bar{e}_o \, |^2 \, , \qquad (3.2a)$$

$$[\, m'^{2}_{mx} \; m'^{2}_{my} \; m'^{2}_{mz} \,]^{T} = \frac{1}{2} \; \bar{C} \, \bar{P}_d \, / \, (k^2 \, | \, \bar{e}_o |^2) \, , \qquad (3.2b)$$

and

$$[\, m'_{exy} \; m'_{eyz} \; m'_{ezx} \,]^{T} = \bar{D} \, \bar{P}_s \, /(4 \; p' \; q') \quad , \qquad (3.2c)$$

$$[\, m'_{mxy} \; m'_{myz} \; m'_{mzx} \,]^{T} = \bar{D} \, \bar{P}_d \, / \, (4 \; p' \; q' \; k^2) \, , \qquad (3.2d)$$

where

$$\bar{C} = \begin{bmatrix} 1 & 1 & -1 & -1 & 1 & 1 \\ 1 & 1 & 1 & 1 & -1 & -1 \\ -1 & -1 & 1 & 1 & 1 & 1 \end{bmatrix} \, , \qquad (3.2e)$$

$$\bar{D} = \begin{bmatrix} 1 & -1 & f & f & -f & -f \\ -f & -f & 1 & -1 & f & f \\ f & f & -f & -f & 1 & -1 \end{bmatrix} \, , \qquad (3.2f)$$

and

$$f = (p'^{2} - q'^{2}) \, / \, | \, \bar{e}_o \, |^2 \, . \qquad (3.2g)$$

The far-field free-space radiation pattern of the EUT is given, in terms of the dipole moments and the cross components, by (Appendix I)

$$P(\theta, \phi) = \frac{15\pi}{r^2 \lambda^2} \{ A_x^2 (\cos^2\theta \cos^2\phi + \sin^2\phi) + A_y^2 (\cos^2\theta \sin^2\phi + \cos^2\phi)$$

$$+ A_z^2 \sin^2\theta - 2 A_{xy} \sin^2\theta \sin\phi \cos\phi - 2 A_{yz} \sin\theta \cos\theta \sin\phi$$

$$- 2 A_{zx} \sin\theta \cos\theta \cos\phi + (B_{xy} - B_{yx}) \cos\theta$$

$$+ (B_{yz} - B_{zy}) \sin\theta \cos\phi + (B_{zx} - B_{xz}) \sin\theta \sin\phi \} \qquad (3.3a)$$

where

$$A^2_\alpha = m'^2_{e\alpha} + k^2 m'^2_{m\alpha} \; ; \; \alpha = x, y, z \qquad (3.3b)$$

$$A_{\alpha\beta} = m'_{e\alpha\beta} + k^2 m'_{m\alpha\beta} ; \; \alpha, \beta = x, y, z \; , \qquad (3.3c)$$

$$B_{\alpha\beta} = 2k m_{e\alpha} m_{m\beta} \sin(\psi_{e\alpha} - \psi_{m\beta}); \quad \alpha, \beta = x, y, z \; . \qquad (3.3d)$$

Note that when the EUT is characterized by three orthogonal electric or magnetic dipoles, $B_{\alpha\beta}$ vanishes. In any event, the total radiated power by the EUT in free space, P_T, is given by:

$$P_T = \int P(\theta, \phi) \, d\Omega = \frac{40\pi^2}{\lambda^2} (A_x^2 + A_y^2 + A_z^2) \; . \qquad (3.4)$$

We note that this method fails, in view of eqs (3.2c) and (3.2d), to give the cross components if p'q' is zero. However, one can always choose the test point (x_o, y_o) and θ_o such that p'q' is nonzero. In a TEM cell possessing symmetry about the yz plane, one would normally choose the test point to lie in this plane ($x_o = 0$) in which case $p = 0$ and for a particular choice of the test point $(0, y_o)$ p'q' will be maximum if θ_o is $\pi/4$. With $x_o = 0$ and $\theta_o = \pi/4$, $p' = q' = q / \sqrt{2}$ and $f = 0$, which simplify the expressions for $\bar{B}$ in eq (3.1c) and $\bar{D}$ in eq (3.2f).

To obtain the absolute values of the dipole moments using the above method we need to know $\bar{e}_o$ which is the normalized field strength, corresponding to the TEM mode, at the test point (x_o, y_o). In the next subsection, we describe four different ways to obtain this normalized field strength defined through the relation

$$\int_s \int \bar{e}_o \times \bar{h}_o \cdot \hat{z} \, ds = 1 \, . \tag{3.5}$$

3.3 Determination of the Normalized Field Strength

3.3.1 Using Theoretical Expression

For simple geometries like circular coaxial or symmetric rectangular coaxial TEM transmission lines, $\bar{e}_o$ may be calculated using the known theoretical expressions. For symmetric rectangular coaxial TEM transmission line, $\bar{e}_o$ is given by [7]:

$$\bar{e}_o(x,y) = \frac{-i \, m' \, dn(m'z) \, \sqrt{Z_o}}{K(\alpha') \, \{P_o(z)\}^{1/2}} \tag{3.6a}$$

$$P_o(z) = \{sn^2(m'w) - sn^2(m'z)\} \tag{3.6b}$$

$$m' = K(k)/a = K(k')/b \tag{3.6c}$$

$$\alpha = sn(m'w,k) \tag{3.6d}$$

$$\alpha' = (1 - \alpha^2)^{1/2} \tag{3.6e}$$

$$z = x + iy \quad , \tag{3.6f}$$

where 2a,2b are the width and the height of the TEM cell; 2w the width of the center conductor; and Z_o, the characteristic impedance of the line. The function K(k) and K(k') are complete elliptic integrals of the first kind of moduli k and k', respectively, where

$$k' = \sqrt{1 - k^2}$$

and sn and dn are Jacobian elliptic functions which may be calculated using the algorithm given in [8]. Amplitude and phase of $\bar{e}_o$ are tabulated in [7] for some typical cell sizes, together with the computer program which generates these values.

3.3.2 Using a Calibrated Probe

If a calibrated field-strength probe is available, $\bar{e}_o$ may simply be obtained by probing the cell at the desired point (x_o,y_o) with unit power at the input port while the other port is terminated with a matched load.

3.3.3 Using a Standard Electric or Magnetic Dipole of Known Strength

With a standard electric dipole, we measure the power outputs P_x and P_y at one port corresponding to the dipole orientations along x- and y-directions, respectively, with the other port terminated with a matched load. Then

$$\bar{e}_o = e_{ox}\,\hat{x} + e_{oy}\,\hat{y}$$

may be obtained through the relations

$$e^2_{ox_{\hat{y}}} = 4P_{x_{\hat{y}}} / m^2_{se} \quad , \tag{3.7}$$

where m_{se} is the known moment of the standard dipole.

With a standard magnetic dipole, we measure the power outputs at one port P_x and P_y corresponding to the dipole orientations along x- and y-directions, respectively, with the other port being terminated with a matched load. Then e_{ox} and e_{oy} are given by

$$e^2_{ox_{\hat{y}}} = 4P_{x_{\hat{y}}} / (k\, m_{sm})^2 \quad , \tag{3.8}$$

where m_{sm} is the known moment of the magnetic dipole.

3.3.4 Using an Uncalibrated Probe with Linear Response

We note that $\bar{e}_o(x_o,y_o)$ represents the field strength at (x_o,y_o) when unit power is flowing across the transmission line and also that the power flow across a TEM transmission line is given by

$$P_{TEM} = \left(\int_C \bar{E} \cdot \overline{d\ell} \right)^2 / Z_o \quad , \tag{3.9}$$

where Z_o is the characteristic impedance of the line, $\overline{E}$ is the electric field strength, and C is any path lying in the cross-sectional plane and extending from the inner conductor to the outer conductor. Using eq (3.9) we may write the normalized field strength $\overline{e}_o(x_o,y_o)$ as

$$\overline{e}_o(x_o,y_o) = \overline{E}(x_o,y_o) \sqrt{Z_o} \Big/ \int_C \overline{E} \cdot \overline{d\ell} \ , \qquad (3.10)$$

which may be measured using an uncalibrated probe since the calibration factor appears both in the numerator and denominator. For doing so, the probe must have a linear response (or else, a calibration of the probe is needed), and the characteristic impedance, Z_o, of the line must be known.

The last expression [eq (3.10)] for $\overline{e}_o$ is an important one since it enables one to extend the measurement procedure to any TEM transmission line geometry for which the theoretical expression for the TEM modal distribution is not available. Though we started with the assumption of an ideal TEM transmission line, we can use the same method even when the transmission line is slightly lossy, as when the cell is lined with absorbing material, or when the inner and outer conductors are made up of imperfect conductors, provided that the TEM nature of the cell is largely unaltered.

The measurement procedure described in this section enables one to determine the magnitudes of the individual electric/magnetic dipole moments along three orthogonal directions and cross components required to obtain the free-space radiation pattern of a composite dipole consisting of three orthogonal electric or magnetic dipoles, each excited with an arbitrary phase. Oftentimes, one is interested in knowing only the total power radiated in free space by the dipole or the EUT. In such a case, we need to take only six measurements, three for the electric dipole and three for the magnetic dipole. In the next section we discuss simple measurement procedures that may be used in such a case.

4. DETERMINATION OF THE TOTAL EMISSION BY AN ELECTRIC AND/OR MAGNETIC DIPOLE USING A SYMMETRIC TEM CELL

In all the measurement procedures that we are going to discuss in this section, we assume that x-, y-, and z-axes refer to a frame of reference fixed with respect to the test cell with the origin at the geometric center, if one exists, of the cell. The point $(x_o,y_o,0)$ refers to the center of the test object with respect to (x,y,z) frame of reference, and x'-, y'-, and z'-axes refer to a frame of reference fixed with respect to the test object with the origin at the center of the test object. In all the cases we assume that the test cell consists of a section of a closed TEM transmission line, symmetric about the yz-plane with perfectly matched transitions at both ends. It is also assumed that the frequency of operation is such that only the dominant TEM mode can propagate. The orthonormal modal function giving the field distribution of the TEM mode is denoted by $\bar{e}_o(x,y)$.

4.1 Electric Dipole Source

Terminating one port of the cell with a matched load, we measure the output powers P_{ex}, P_{ey}, and P_{ez} at the other port corresponding to the orientations of the test object given by (x'→y), (y'→y), and (z'→y), respectively. Since $\bar{e}_o$ has only the y-component at the test point, the electric dipole moments are given by

$$m'^2_{ei} = 4\, P_{ei} \,/\, |\bar{e}_o|^2 \;;\; i = x,y,z \;. \tag{4.1}$$

The total power P_{Te} radiated in free space is given by

$$P_{Te} = 40\pi^2 (m'^2_{ex} + m'^2_{ey} + m'^2_{ez}) \,/\, \lambda^2 \;, \tag{4.2}$$

where λ is the wavelength of operating frequency.

4.2 Magnetic Dipole Source

Terminating one port of the cell with a matched load, we measure the power outputs P_{mx}, P_{my}, and P_{mz} at the other port corresponding to the orientations of the test object given by $(x' \rightarrow x)$, $(y' \rightarrow x)$, $(z' \rightarrow x)$, respectively. Then the magnetic dipole moments are given by

$$m'^2_{mi} = 4\, P_{mi} \,/\, (k\, |\bar{e}_o|)^2 \;;\; i = x,y,z \;. \tag{4.3}$$

The total power P_{Tm} radiated in free space is given by

$$P_{Tm} = 160\, \pi^4 (m'^2_{mx} + m'^2_{my} + m'^2_{mz}) \,/\, \lambda^4 \;. \tag{4.4}$$

4.3 Composite Source Consisting of Electric and Magnetic Dipoles

When the source consists of electric and magnetic dipoles, we need to make measurements of sum and difference powers as shown in figure 3. We measure the powers P_{si} and P_{di}, $i = x,y,z$ at the sum and difference ports corresponding to the orientations of the test object given by $(z' \rightarrow x,\ x' \rightarrow y)$, $(x' \rightarrow x,\ y' \rightarrow y)$, and $(y' \rightarrow x,\ z' \rightarrow y)$, respectively. Then we have

$$m'^2_{ei} = P_{si} \,/\, |\bar{e}_o|^2 \;, \qquad i = x,\ y,\ z \tag{4.5}$$

$$m'^2_{\substack{mx \\ y \\ z}} = P_{\substack{dy \\ z \\ x}} \,/\, (k\, |\bar{e}_o|)^2 \;. \tag{4.6}$$

The total radiated power P_T, in free space, is given by $P_T = P_{Te} + P_{Tm}$ where P_{Te} and P_{Tm} may be obtained from eqs (4.2) and (4.4).

In all the cases discussed, we need the value of $\bar{e}_o$ at the test point. This may be obtained using any of the four methods given in Section 3.3.

So far, we have assumed that the test cell consists of a section of TEM transmission line with perfectly matched transitions at both ends. However, if the test cell is made of a section of waveguide that cannot support a TEM mode, the modal function corresponding to the fundamental mode may also have a z-component in which case the simple relation of the form in eq (2.8) is no longer true. As a result, it is not possible to decompose the electric and magnetic dipoles using the sum and difference technique that we discussed in this section and the previous section. When the EUT can be characterized entirely by dipoles of the electric or magnetic type but not of both types, it is still possible to obtain the x-, y-, and z-components of the dipole by a modified procedure that is described in Appendix II.

5. THE EFFECT OF MISMATCHED TRANSITIONS

In the preceding sections we assumed that the test cell has a section of uniform transmission line with perfectly matched transitions at both ends. If the transitions are not matched, we need to modify the measurement procedure to account for the mismatches introduced by the transitions. In this section, we describe such a measurement scheme under the assumption that the transitions are lossless and reciprocal, which is true in almost all the practical situations. First, we note that, as shown in Appendix III, any lossless reciprocal two-port network may be represented by an equivalent circuit consisting of two sections of lossless lines coupled by an ideal transformer. A TEM cell with mismatched transitions may thus be represented by the equivalent circuit shown in figure 9 where the equivalent circuits corresponding to the transitions are enclosed by dotted lines. In this equivalent circuit, L represents the length of the transmission line section of the cell excluding the

transitions. The output connectors are assumed to have the same characteristic impedance as that of the transmission line section of the cell. In Appendix IV, we derive the matrix equations relating the complex amplitudes a and b given by eq (2.10a) and the complex amplitudes $\tilde{a}$ and $\tilde{b}$ that would be measured using a cell with mismatched transitions. Using the relation of eq (A4.5a) for the case when the radiator is located midway between the cell (z = 0), we obtain the following equation using straightforward algebraic manipulations:

$$|a \pm b|^2 = |F_{\pm}|^2 \, |(\tilde{a} \pm G\,\tilde{b})|^2 \tag{5.1a}$$

where

$$F_{\pm} = \left(\frac{n_a^2 + 1}{2n_a} \right) \left(e^{ik\ell'_{1a}} \pm \frac{1 - n_b^2}{1 + n_b^2} \, e^{-ik\ell'_{1a}} \right) \tag{5.1b}$$

$$G = \frac{n_a(n_b^2 + 1)}{n_b(n_a^2 + 1)} \, e^{ik(\ell_{2b} - \ell_{2a})} \left(e^{ik\ell'_{1b}} \pm \frac{1 - n_a^2}{1 + n_a^2} \, e^{-ik\ell'_{1b}} \right) \tag{5.1c}$$

$$\div \left(e^{ik\ell'_{1a}} \pm \frac{1 - n_b^2}{1 + n_b^2} \, e^{-ik\ell'_{1a}} \right) ,$$

$$\ell'_{\substack{1a \\ b}} = \ell_{\substack{1a \\ b}} + \tfrac{1}{2} L \tag{5.1d}$$

and the circuit parameters ℓ_{1a}, ℓ_{1b}, ℓ_{2a}, ℓ_{2b}, n_a, n_b, and L are shown in figure 9. Based upon eq (5.1a), we describe the methods of accounting for the mismatched transitions depending upon whether the transitions are identical or not.

5.1 Cell with Identical Transitions

If the cell has identical transitions the quantity G in eq (5.1c) reduces to unity. For a specific orientation of the test object, the true sum and difference powers $P_{\substack{s \\ d}}$ corresponding to matched transitions are obtained in terms of the measured sum and difference powers $\tilde{P}_{\substack{s \\ d}}$ with mismatched transitions, through the following relation

$$P_{\substack{s \\ d}} = |F_{\pm}|^2 \tilde{P}_{\substack{s \\ d}} \qquad (5.2)$$

with $n_a = n_b = 1$ and $\ell_{1a} = \ell_{1b} = \ell_1$.

5.2 Cell with Dissimilar Transitions

If the cell has dissimilar transitions, simple sum and difference power measurement does not give enough information to obtain the true sum and difference powers corresponding to matched transitions. To obtain the latter, we use the following modified procedure:

We connect an attenuator and phase shifter in the negative port (see fig. 9) before taking the sum and difference. The attenuation in dB is given by -20 log |G| and the required phase shift by $\angle G$. Then the true sum and difference powers are expressed in terms of the measured sum and difference power through the same relation in eq (5.2) with F being given by eq (5.1b). If $|G| > 1$, then we connect the attenuator and the phase shifter in the positive port with the subscripts a and b interchanged.

When making measurements with a cell having mismatched transitions, we should note that it is not possible to obtain the sum/difference power at one port by short circuiting the other port at odd/even number of quarter wavelengths. Further, even when the source is made of only electric or magnetic dipoles, we cannot make measurements at one port with the other port terminated by a matched load. We need to use the general

procedure outlined in section 3 with the modifications discussed above. It is also obvious that we need to know the equivalent circuit parameters of the transitions to account for their effect. In what follows, we describe a measurement procedure to determine these parameters.

5.3 Measurement of Equivalent Circuit Parameters of the Transitions

The measurement of the equivalent circuit parameters of the transitions is complicated by the fact that the transitions are integral parts of the TEM cell and, in practice, it is not possible to isolate them from the cell for the purpose of measuring the circuit parameters of the individual transitions. Any external measurements on the cell can only provide the equivalent circuit parameters of the complete cell including both transitions. As will be clear later, whereas the complete cell may be characterized by only three independent real parameters (two in the case of identical transitions), we need six independent parameters (three in the case of identical transitions) to individually characterize the transitions. Thus it is not possible to obtain the equivalent circuit parameters of the transitions by external measurements alone, by which we mean without a probe or a standard radiator inside the cell. However, it is possible to completely characterize the transitions by making measurements with a standard radiator inside the cell and combining these results with the equivalent circuit parameters of the complete cell which may be obtained through external measurements alone. In what follows we describe a step-by-step procedure of obtaining the equivalent circuit parameters of the transitions. The required analytic details are given in Appendices IV and V. We treat the case of identical transitions separately from that of dissimilar transitions.

5.3.1 Cell with Identical Transitions

If the cell has identical transitions, the parameters $\ell_{1a} = \ell_{1b} = \ell_1$, $\ell_{2a} = \ell_{2b} = \ell_2$, and $n_a = n_b = n$ will completely characterize the transitions. To obtain these parameters we proceed as follows:

1. Measure the cascading matrix $\overline{R}$ of the entire cell using any standard method [6]. Because of the symmetry of the cell, the cascading parameters R_{12}, R_{21}, and R_{22} are related to R_{11} through

$$R_{12} = R_{21} = (R_{11}\, R_{11}^{*} - 1)^{1/2} \tag{5.3a}$$

and

$$R_{22} = R_{11}^{*} \,. \tag{5.3b}$$

2. Terminate the negative port of the TEM cell with a matched load corresponding to the characteristic impedance of the transmission line section of the cell and measure the complex ratio of the voltages $\tilde{a}(+g)$ and $\tilde{a}(-g)$ across a matched detector at the positive port with a standard electric dipole placed inside the cell in transverse planes $z = +g$ and $z = -g$, respectively (fig. 9), where g is a convenient value. To obtain maximum sensitivity, the dipole must be aligned with the vertical E-field inside the cell.

3. Calculate the real parameters n and ℓ_1 using the following relation which is based upon eq (A4.7):

$$\left(\frac{1-n^2}{1+n^2}\right) e^{-ik\ell_1} = \left\{ i\left(\frac{\tilde{a}_r\, e^{i2kg_{+1}}}{\tilde{a}_r\, e^{i2kg_{-1}}}\right) \sin(2kg) - \cos(2kg) \right\} e^{ikL}, \tag{5.4a}$$

(5.4a)

where

$$\tilde{a}_r = \tilde{a}(+g) \;/\; \tilde{a}(-g) \quad . \tag{5.4b}$$

After obtaining n, we proceed to calculate ℓ_2 using eq (A5.2a),

$$\begin{bmatrix} \sin(2k\ell_2) \\ \cos(2k\ell_2) \end{bmatrix} = \frac{2n^2}{\Delta} \begin{bmatrix} -(1+n^4)\sin kL' & -2n^2 \cos kL' \\ 2n^2 \cos kL' & -(1+n^4)\sin kL' \end{bmatrix} \begin{bmatrix} R_e(R_{11}) \\ I_m(R_{11}) \end{bmatrix} \tag{5.5a}$$

where

$$\Delta = 4n^4 \cos^2 kL' + (1+n^2)^2 \sin^2 kL' \;, \tag{5.5b}$$

and

$$L' = 2\ell_1 + L \;. \tag{5.5c}$$

We note that the parameter ℓ_2 is not needed in calculating the correction factor, F. Thus it is not necessary to measure the cascading parameter R_{11} of the entire cell unless one is interested in obtaining the complete scattering/cascading matrix of the transition.

5.3.2 Cell with Dissimilar Transitions

If the cell has dissimilar transitions, we essentially follow the same procedure as discussed above except that we repeat step 2 on both ports. The calculation procedure is also slightly more complicated as described below.

1. Measure the cascading matrix $\overline{R}$ of the complete cell.

Since the cell has dissimilar transitions, the relations in eqs (5.3a) and (5.3b) are now replaced by the following more restrictive relations which follow from the lossless and reciprocal nature of the cell.

$$R_{12} = R_{21}^* \tag{5.6a}$$

$$R_{11} = R_{22}^* \tag{5.6b}$$

$$R_{11} R_{22} - R_{12} R_{21} = 1 \ . \tag{5.6c}$$

2. Terminate the negative port of the cell with a matched load and measure the complex ratio of the voltages $\tilde{a}(+g)$ and $\tilde{a}(-g)$ across a matched detector at the positive port with a standard electric dipole placed inside the cell at $z = +g$ and $z = -g$, respectively.

3. Terminate the positive port of the cell with a matched load and measure the complex ratio of the voltage $\tilde{b}(-g)$ and $\tilde{b}(+g)$ across a matched detector at the negative port with the standard electric dipole placed at $z = -g$ and $z = +g$, respectively.

4. Calculate the real parameters, n_a, ℓ_{1a}, n_b, and ℓ_{1b}, using the following relations which are derived in Appendix IV

$$\frac{1-n_a^2}{1+n_a^2} \ e^{-i2k\ell_{1a}} = \left\{ i\left(\frac{\tilde{b}_r \exp(i2kg)+1}{\tilde{b}_r \exp(i2kg)-1}\right) \sin(2kg) - \cos(2kg) \right\} e^{ikL} \tag{5.7a}$$

$$\frac{1-n_b^2}{1+n_b^2} \ e^{i2k\ell_{1b}} = \left\{ i\left(\frac{\tilde{a}_r \exp(i2kg)+1}{\tilde{a}_r \exp(i2kg)-1}\right) \sin(2kg) - \cos(2kg) \right\} e^{ikL} \tag{5.7b}$$

where

$$\tilde{a}_r = \tilde{a}(+g) \;/\; \tilde{a}(-g) \;, \qquad (5.7c)$$

and

$$\tilde{b}_r = \tilde{b}(-g) \;/\; \tilde{b}(+g) \;. \qquad (5.7d)$$

5. Having known n_a, ℓ_{1a}, n_b, and ℓ_{1b}, we then calculate $\begin{matrix}\sin\\ \cos\end{matrix} k(\ell_{2a} + \ell_{2b})$ and $\begin{matrix}\sin\\ \cos\end{matrix} k(\ell_{2a} - \ell_{2b})$ using eq (A.5), and hence determine ℓ_{2a} and ℓ_{2b} uniquely.

6. EXPERIMENTAL RESULTS

To verify the theoretical analysis presented in previous sections, some measurements were made using a symmetric rectangular coaxial TEM cell of dimensions 1.20x1.20x2.40 m^3 as shown in figure 5, and a center conductor of width 99.2 cm. The cell has matched transitions at boths ends and is partially loaded with absorbing material, as shown in figure 6, to suppress the higher-order modes at high frequencies. A spherical dipole radiator having a radius of 5 cm was used as the test source. The radiator consists of two hemispherical shells which are fed at the poles and held together by threading onto a dielectric disc such that there is a gap of 3 mm between them. The electronic circuitry feeding the dipole is enclosed within the shells and consists of a battery-operated power supply and a 30-MHz crystal oscillator followed by an amplifier. Thus, the radiator is self-contained and no external connections are needed. The spherical dipole radiator and the TEM cell were developed at NBS by M. Crawford. Earlier measurements indicated that the characteristic impedance of the cell remained unaltered after placing the absorbing material. However, measurements with a short probe indicated that the normalized field distribution is different from the theoretical distribution corresponding to an unloaded cell. In figure 7 we have plotted the theoretical distribution using eq (3.6) and the measured distribution along the vertical axis of the cell.

Two sets of measurements were made. In one experiment, the dipole was placed such that it was aligned with the vertical axis of the cell, and the dipole moment was measured using our technique at various test points along the y-axis of the cell to see if the dipole moment is sensitive to changes in the impedance of the surrounding medium. Table I gives the computed values of the dipole moment as a function of the vertical distance y_o of the test point from the center conductor. As we can see from the table, there is no appreciable change in dipole moment as the test point is moved along the vertical axis.

In the second experiment, the x-, y-, and z-components of the dipole were measured using our technique for various orientations of the dipole radiator, and from these measurements the (θ,ϕ) coordinates of the dipole vector were computed and compared with the actual orientations of the dipole. The results are tabulated in Table II. From these results we note that the measured (θ,ϕ) coordinates of the dipole vector are close to the actual values within $\pm 1°$. Also, the spread in the measured dipole moment (Table I) is within ± 2.5 percent, thus establishing the usefulness and validity of our method for the case of an electric dipole source.

At the time of writing this report, a magnetic dipole source was not available, and hence it was not possible to test our method for the case of a magnetic dipole source or a composite source.

Table I. Measured dipole moment vs. the height of the test point from the center conductor.

Y_o (cm)	$\lvert\bar{m}_e\rvert^+$	$\lvert\bar{m}_e\rvert^{++}$
	Dipole Moment (Amp. Meter x 10^{-4})	
15	2.983	2.740
20	2.916	2.705
25	2.830	2.711
30	2.736	2.708
35	2.647	2.728
40	2.531	2.645
45	2.418	2.606
50	2.333	2.625

$^+$Using theoretical $e_o(0,y_o)$ corresponding to unloaded cell.

$^{++}$Using experimental $e_o(0,y_o)$ measured with high impedance probe.

Table II. Measured dipole orientations compared with actual dipole orientations.

Y_o (cm)	Measured θ, ϕ (deg.) ($\theta_o = 45^0$)	Measured θ, ϕ (deg.) ($\theta_o = 0^0$)	Actual θ, ϕ (deg.)
20	62.94, 60.38	62.19, 59.36	61.4, 58.4
30	63.11, 58.61	60.00, 56.55	61.4, 58.4
40	63.10, 58.16	62.90, 60.37	61.4, 58.4
20	66.79, 69.73	65.28, 70.98	65.36, 72.19
20	73.77, 136.97	73.59, 136.32	72.81, 136.98
20	48.57, -55.35	49.27, -53.92	47.60, -54.19
30	44.21, 140.14	44.68, -144.70	42.67, -139.27
30	76.60, -40.88	80.59, -41.87	80.83, -41.14

7. CONCLUSIONS

Experimental procedures described in the report should enable one to determine the total power radiated in free space by (and/or the complete free space-radiation pattern of) an electrically small radiating object that may be characterized by a system of elementary dipole radiators consisting of three orthogonal electric dipoles or three orthogonal magnetic dipoles, each excited with arbitrary phase. The test cell is not restricted to a specific geometry as long as it can support a TEM mode and the dimensions are such that no higher-order mode can propagate at the test frequency. The discussion presented in section 5 should enable one to extend the measurement procedure to test cells with mismatched end transitions.

The experimental results presented in section 6 demonstrate the validity of our test procedure for the case of an electric dipole source. It is reasonable to assume that the same will be true for the case of a magnetic dipole source. However, for the case of a composite source, we need to establish the usefulness of our method through actual measurements. We plan to do this in the near future.

8. ACKNOWLEDGMENTS

The authors are very thankful to M. L. Crawford and J. L. Workman for their assistance during the course of the experimental work. Also, their permission to use the spherical dipole radiator and the TEM cell is gratefully acknowledged. Thanks are also due to Dr. M. Kanda for the technical discussions we had with him during the course of this study. The continued and wholehearted support and encouragement from C. K. S. Miller and F. X. Ries are acknowledged with appreciation.

9. REFERENCES

[1] Adams, J. W., Electromagnetic interference measurement program at the National Bureau of Standards, USNC/URSI, Commissions I-VIII, Annual Meeting Digest, p. 33 (Oct. 20-23, 1975).

[2] Crawford, M. L., Generation of standard EM fields using TEM transmission cells, IEEE Trans. on Electromag. Compat. EMC-16, No. 4, 189-195 (Nov. 1974).

[3] Crawford, M. L., Workman, J. L., and Thomas, C. L., Generation of EM susceptibility test fields using a large absorber-loaded TEM cell, IEEE Trans. on Instrum. and Measure. IM-26, No. 3, 225-230 (Sept. 1977).

[4] Crawford, M. L., and Workman, J. L., Asymmetric versus symmetric TEM cells for EMI measurements, Conference Rept. IEEE Inter. Symp. on EMC, 204-210, Atlanta, GA (June 20-22, 1978).

[5] Crawford, M. L., Workman, J. L., and Thomas, C. L., Expanding the bandwidth of TEM cells for EMC measurements, IEEE Trans. on Electromag. Compat. EMC-20, No. 3, 368-375 (Aug. 1978).

[6] Collin, R. E., Field Theory of Guided Waves (New York, McGraw-Hill Book Company, 1960).

[7] Tippet, J. C., and Chang, D. C., Radiation characteristics of electrically small devices in a TEM transmission cell, IEEE Trans. on Electromag. Compat. EMC-18, No. 4, 134-140 (Nov. 1976).

[8] Tippet, J. C., and Chang, D. C., Radiation characteristics of dipole sources located inside a rectangular, coaxial transmission line, NBSIR 75-829 (Jan. 1976).

[9] Ghose, R. N., Microwave Circuit Theory and Analysis (New York, McGraw-Hill Book Company, 1963).

[10] Kerns, D. M., and Beatty, R. W., Basic Theory of Waveguide Junctions and Introductory Microwave Network Analysis, pp. 41-48 (New York, Pergamon Press, 1967).

APPENDIX I

FAR-FIELD RADIATION PATTERN OF A SYSTEM OF ORTHOGONAL, ELECTRIC- AND MAGNETIC-DIPOLE SOURCES EXCITED WITH ARBITRARY PHASES

Consider a system of short, electric- and magnetic-dipole sources with moments $m_{\substack{ex \\ m}}$, $m_{\substack{ey \\ m}}$ and $m_{\substack{ez \\ m}}$ along the x,y,z axes and excited with phases $\psi_{\substack{ex \\ m}}$, $\psi_{\substack{ey \\ m}}$, $\psi_{\substack{ez \\ m}}$, respectively.

Let $\overline{M}_e$ and $\overline{M}_m$ be the complex moment vectors given by

$$\overline{M}_{\substack{e \\ m}} = \hat{x}\, m_{\substack{ex \\ m}}\, e^{i\psi_{\substack{ex \\ m}}} + \hat{y}\, m_{\substack{ey \\ m}}\, e^{i\psi_{\substack{ey \\ m}}} + \hat{z}\, m_{\substack{ez \\ m}}\, e^{i\psi_{\substack{ez \\ m}}} \qquad (A1.1)$$

The complex vector potential $\overline{A}$ due to the electric dipole system is then given by

$$\overline{A} = \overline{M}_e \frac{\mu_o}{4\pi} \frac{e^{-ikr}}{r} \qquad (A1.2)$$

where r is the distance from the dipole source. We use the relation between the cartesian and the spherical coordinate system

$$\begin{pmatrix} \hat{x} \\ \hat{y} \\ \hat{z} \end{pmatrix} = \begin{pmatrix} \sin\theta\cos\phi & \cos\theta\cos\phi & -\sin\phi \\ \sin\theta\sin\phi & \cos\theta\sin\phi & \cos\phi \\ \cos\theta & -\sin\theta & 0 \end{pmatrix} \begin{pmatrix} \hat{r} \\ \hat{\theta} \\ \hat{\phi} \end{pmatrix} \qquad (A1.3)$$

and write the components of $\overline{A}$ as

$$A_r = (M_{ex} \sin\theta \cos\phi + M_{ey} \sin\theta \sin\phi + M_{ez}\cos\theta)\ (\mu_o/4\pi)e^{-ikr}/r \qquad (A1.4a)$$

$$A_\theta = (M_{ex} \cos\theta \cos\phi + M_{ey} \cos\theta \sin\phi - M_{ez} \sin\theta)\ (\mu_o/4\pi)e^{-ikr}/r \qquad (A1.4b)$$

$$A_\phi = (-M_{ex} \sin\phi + M_{ey} \cos\phi)\ (\mu_o/4\pi)e^{-ikr}/r \qquad (A1.4c)$$

where we have defined

$$M_{\substack{ex\\y\\z}} = m_{\substack{ex\\y\\z}} \exp\ (i\psi_{\substack{ex\\y\\z}}) \qquad (A1.4d)$$

Using the relations

$$\bar{H} = (\nabla \times \bar{A})\ /\mu_o \qquad (A1.5a)$$

$$\bar{E} = \frac{-i\omega}{k^2} \nabla\ (\nabla \cdot \bar{A})\ -i\omega\bar{A} \qquad (A1.5b)$$

and retaining only those terms which decay as $1/r$, we find that

$$H_\theta = (-M_{ex} \sin\phi + M_{ey} \cos\phi)\ (\frac{ik}{4\pi r})\ \exp\ (-ikr) \qquad (A1.6a)$$

$$H_\phi = (M_{ex} \cos\theta \cos\phi + M_{ey} \cos\theta \sin\phi - M_{ez} \sin\theta)\ (\frac{-ik}{4\pi r})\ \exp\ (-ikr) \qquad (A1.6b)$$

$$E_\theta = \zeta_o H_\phi \qquad (A1.6c)$$

$$E_\phi = -\zeta_o H_\theta \qquad \text{(A1.6d)}$$

where

$$\zeta_o = \sqrt{\mu_o/\varepsilon_o} \cong 120\pi \ . \qquad \text{(A1.6e)}$$

Using the duality principle, we could write down the electric- and magnetic-field components E'_θ, E'_ϕ, H'_θ, and H'_ϕ due to an orthogonal system of magnetic dipoles with moments m_{mx}, m_{my}, m_{mz}, and phases ψ_{mx}, ψ_{my}, ψ_{mz} as

$$E'_\theta = (-M_{mx} \sin\phi + M_{my} \cos\phi)\left(\frac{\omega\mu_o k}{4\pi r}\right) \exp(-ikr) \qquad \text{(A1.7a)}$$

$$E'_\phi = (M_{mx}\cos\theta\cos\phi + M_{my}\cos\theta\sin\phi - M_{mz}\sin\theta)\left(\frac{-\omega\mu_o k}{4\pi r}\right) \exp(-ikr) \qquad \text{(A1.7b)}$$

$$H'_\theta = -E'_\phi/\zeta_o \qquad \text{(A1.7c)}$$

$$H'_\phi = E'_\theta/\zeta_o \qquad \text{(A1.7d)}$$

where we have defined

$$M_{\substack{mx\\y\\z}} = m_{\substack{mx\\y\\z}} \exp\left(i\psi_{\substack{mx\\y\\z}}\right) . \qquad \text{(A1.8)}$$

The total fields, due to the combined presence of electric and magnetic dipoles, are then given by

$$E^t_\theta = E_\theta + E'_\theta = (\tilde{M}_{e\theta} + ik\tilde{M}_{m\phi})\left(\frac{-i\omega\mu_o}{4\pi r}\right) e^{-ikr} \ , \qquad \text{(A1.9a)}$$

$$E^t_\phi = E_\phi + E'_\phi = (\tilde{M}_{e\phi} - ik\tilde{M}_{m\theta})\left(\frac{-i\omega\mu_o}{4\pi r}\right) e^{-ikr} \ , \qquad \text{(A1.9b)}$$

$$H^t_\theta = \mp E^t_\phi/\zeta_o \quad , \qquad \text{(A1.9c)}$$

where we have defined

$$\tilde{M}_{e\theta} = M_{ex} \cos\theta \cos\phi + M_{ey} \cos\theta \sin\phi - M_{ez} \sin\theta, \qquad \text{(A1.10a)}$$

and

$$\tilde{M}_{e\phi} = -M_{ex} \sin\phi + M_{ey} \cos\phi \ . \qquad \text{(A1.10b)}$$

The time-averaged, radiated power per unit solid angle, $P(\theta,\phi)$, is given by

$$P(\theta,\phi) = \tfrac{1}{2} \{E^t_\theta E^{t*}_\theta + E^t_\phi E^{t*}_\phi\}/\zeta_o \ , \qquad \text{(A1.11)}$$

which, upon using eqs (A1.9a) and (A1.9b), becomes

$$P(\theta,\phi) = \frac{\zeta_o}{8r^2\lambda^2} \{|\tilde{M}_{e\theta}|^2 + |\tilde{M}_{e\phi}|^2 + k^2 (|\tilde{M}_{m\theta}|^2 + |\tilde{M}_{m\phi}|^2)$$

$$+ ik [\tilde{M}_{m\phi} \tilde{M}^*_{e\theta} - \tilde{M}_{e\theta} \tilde{M}^*_{m\phi} + \tilde{M}_{e\phi} \tilde{M}^*_{m\theta} - \tilde{M}_{m\theta} \tilde{M}^*_{e\phi}]\} \qquad \text{(A1.12)}$$

where λ is the wavelength at the operating frequency.

By substituting for $\tilde{M}_{e\theta}$, $\tilde{M}_{e\phi}$ from eq (A1.10) and noting the definitions in eqs (A1.4d) and (A1.8), we obtain

$$P(\theta,\phi) = \frac{\zeta_o}{8r^2\lambda^2} [(m^2_{ex} + k^2 m^2_{mx}) (\cos^2\theta \cos^2\phi + \sin^2\phi)$$

$$+ (m^2_{ey} + k^2 m^2_{my}) (\cos^2\theta \sin^2\phi + \cos^2\phi) + (m^2_{ez} + k^2 m^2_{mz}) \sin^2\theta$$

$$- 2\{m_{ex}m_{ey}\cos(\psi_{ex}-\psi_{ey}) + k^2 m_{mx}m_{my}\cos(\psi_{mx} - \psi_{my})\} \sin^2\theta \sin\phi \cos\phi$$

$$- 2\{m_{ey}\, m_{ez}\, \cos(\psi_{ey}-\psi_{ez}) + k^2 m_{my}\, m_{mz}\, \cos(\psi_{my}-\psi_{mz})\} \sin\theta \cos\theta \sin\phi$$

$$- 2\{m_{ez}m_{ex}\cos(\psi_{ez} - \psi_{ex}) + k^2 m_{mz}\, m_{mx}\, \cos(\psi_{mz} - \psi_{mx})\} \sin\theta \cos\theta \cos\phi$$

$$+ 2k\{m_{ex}m_{my}\, \sin(\psi_{ex}- \psi_{my}) - m_{ey}m_{mx}\, \sin(\psi_{ey}- \psi_{mx})\} \cos\theta$$

$$+ 2k\{m_{ey}m_{mz}\, \sin(\psi_{ey}- \psi_{mz}) - m_{ez}m_{my}\, \sin(\psi_{ez}- \psi_{my})\} \sin\theta \cos\phi$$

$$+ 2k\{m_{ez}m_{mx}\, \sin(\psi_{ez}- \psi_{mx}) - m_{ex}m_{mz}\, \sin(\psi_{ex}- \psi_{mz})\} \sin\theta \sin\phi] \; . \qquad \text{(A1.13)}$$

The total radiated power P_T is given by

$$P_T = \int P(\theta,\phi)\, d\Omega$$

$$= \frac{40\pi^2}{\lambda^2} \{m_{ex}^2 + m_{ey}^2 + m_{ez}^2 + k^2\, (m_{mx}^2 + m_{my}^2 + m_{mz}^2)\} \qquad \text{(A1.14)}$$

where we have made use of the fact that $\zeta_o \cong 120\pi$.

APPENDIX II

MEASUREMENT WITH A TEST CELL THAT CANNOT SUPPORT TEM MODE

If the waveguide section of the test cell cannot support TEM mode, the electric field corresponding to the fundamental mode may also have a z-component, and, as a result, it is not possible to decompose the electric and magnetic dipoles using the sum and difference technique discussed in sections 3 and 4. However, if the source is entirely made of electric or magnetic dipoles, it is still possible to obtain the x,y,z-components of the dipole by the following procedure:

Terminate one port of the cell with a matched load and measure output powers P_i, i = 1,2...,6, at the other port, for the orientations of the test object given by (x'→x, y'→y), (x'→x, y'→-y), (y'→x, z'→y), (y'→x, z'→-y), (z'→x, x'→y), and (z'→x, x'→-y), respectively. Then, from eqs (2.5) and (2.6), we have

$$p^2M_1^2+ q^2M_2^2+ r^2M_3^2+ 2pqM_{12}+ 2qrM_{23}+ 2rpM_{31}= P_1 \quad \text{(A2.1a)}$$

$$p^2M_1^2+ q^2M_2^2+ r^2M_3^2- 2pqM_{12}+ 2qrM_{23}- 2rpM_{31}= P_2 \quad \text{(A2.1b)}$$

$$p^2M_2^2+ q^2M_3^2+ r^2M_1^2+ 2pqM_{23}+ 2qrM_{31}+ 2rpM_{12}= P_3 \quad \text{(A2.1c)}$$

$$p^2M_2^2+ q^2M_3^2+ r^2M_1^2- 2pqM_{23}+ 2qrM_{31}- 2rpM_{12}= P_4 \quad \text{(A2.1d)}$$

$$p^2M_3^2+ q^2M_1^2+ r^2M_2^2+ 2pqM_{31}+ 2qrM_{12}+ 2rpM_{23}= P_5 \quad \text{(A2.1e)}$$

$$p^2M_3^2 + q^2M_1^2 + r^2M_2^2 - 2pqM_{31} + 2qrM_{12} - 2rpM_{23} = P_6 \ , \quad \text{(A2.1f)}$$

where we have used the following notation:

(a) for an electric dipole source,

$$\begin{matrix} M_1 \\ 2 \\ 3 \end{matrix} = \begin{matrix} m_{ex} \\ y \\ z \end{matrix} \quad \text{(A2.2a)}$$

$$p = e_{ox}; \quad q = e_{oy}; \quad r = e_{oz} \quad \text{(A2.2b)}$$

$$M_{12} = m_{ex}\, m_{ey} \cos(\psi_{ex} - \psi_{ey}), \quad \text{etc.} \quad \text{(A2.2c)}$$

(b) for a magnetic dipole source,

$$\begin{matrix} M_1 \\ 2 \\ 3 \end{matrix} = \omega\mu_o \begin{matrix} m_{mx} \\ y \\ z \end{matrix} \quad \text{(A2.3a)}$$

$$p = h_{ox}; \quad q = h_{oy}; \quad r = h_{oz} \quad \text{(A2.3b)}$$

$$M_{12} = \omega^2\mu_o^2\, m_{mx}\, m_{my} \cos(\psi_{mx} - \psi_{my}), \text{ etc.} \quad \text{(A2.3c)}$$

The solution to eqs (A2.1a)--(A2.1f) is given by

$$\begin{pmatrix} M_{12} \\ M_{23} \\ M_{31} \end{pmatrix} = \frac{1}{4p\Delta_1} \begin{pmatrix} q^2 & r^2 & -qr \\ -qr & q^2 & r^2 \\ r^2 & -qr & q^2 \end{pmatrix} \begin{pmatrix} P_1 - P_2 \\ P_3 - P_4 \\ P_5 - P_6 \end{pmatrix} \quad \text{(A2.4)}$$

$$\begin{pmatrix} M_1^2 \\ M_2^2 \\ M_3^2 \end{pmatrix} = \frac{1}{\Delta_2} \begin{pmatrix} p^4 - q^2r^2 & r^4 - p^2q^2 & q^4 - r^2p^2 \\ q^4 - r^2p^2 & p^4 - q^2r^2 & r^4 - p^2q^2 \\ r^4 - p^2q^2 & q^4 - r^2p^2 & p^4 - q^2r^2 \end{pmatrix} \begin{pmatrix} B_1 \\ B_2 \\ B_3 \end{pmatrix} , \qquad \text{(A2.5)}$$

where

$$\Delta_1 = q^3 + r^3 , \qquad \text{(A2.6a)}$$

$$\Delta_2 = p^6 + q^6 + r^6 - 3p^2q^2r^2 , \qquad \text{(A2.6b)}$$

$$B_1 = \tfrac{1}{2} (P_1 + P_2) - 2qrM_{23} , \qquad \text{(A2.7a)}$$

$$B_2 = \tfrac{1}{2} (P_3 + P_4) - 2qr\, M_{31} , \qquad \text{(A2.7b)}$$

and

$$B_3 = \tfrac{1}{2} (P_5 + P_6) - 2qr\, M_{12} . \qquad \text{(A2.7c)}$$

The normalized components of modal fields e_{ox}, e_{oy}, e_{oz}, h_{ox}, h_{oy}, and h_{oz} must either be known theoretically or be measured using a calibrated probe.

APPENDIX III

EQUIVALENT CIRCUIT OF AN ARBITRARY, LOSSLESS, RECIPROCAL TWO-PORT NETWORK

The scattering matrix of a lossless, reciprocal junction has the following symmetry and unitary properties [9]:

$$\bar{S} = \bar{S}^{T} \tag{A3.1a}$$

$$\bar{S}\ \bar{S}^{T*} = \bar{I}\ , \tag{A3.1b}$$

where $\bar{I}$ is the unit matrix and all the ports of the junction are assumed to have the same characteristic impedance.

Using the above relations, the scattering matrix of a 2-port lossless, reciprocal network may be written as [10]

$$\bar{S} = \begin{pmatrix} S_{11} & \sqrt{1 - S_{11}S_{11}^{*}}\ e^{i\psi_{12}} \\ \sqrt{1 - S_{11}S_{11}^{*}}\ e^{i\psi_{12}} & |S_{11}|\ e^{i\psi_{22}} \end{pmatrix} \tag{A3.2a}$$

with ψ_{12} being given in terms of ψ_{11} and ψ_{22} by

$$\psi_{12} = \tfrac{1}{2}(\psi_{11} + \psi_{22}) + N_{o}\,\pi/2\ , \tag{A3.2b}$$

where N_{o} is an odd integer and ψ_{pq} is the phase of S_{pq}.

We show that such a two-port may be represented by the equivalent circuit shown in figure 8, which consists of two sections of lossless, transmission lines coupled by a transformer. To do this, we first obtain the cascading

matrix $\overline{R}$ of this equivalent circuit as the product of the cascading matrices of the individual sections as follows:

$$\overline{R} = \begin{pmatrix} e^{-ik\ell_1} & 0 \\ 0 & e^{ik\ell_1} \end{pmatrix} \frac{1}{2n} \begin{pmatrix} (n^2+1) & (1-n^2) \\ (1-n^2) & (n^2+1) \end{pmatrix} \begin{pmatrix} e^{-ik\ell_2} & 0 \\ 0 & e^{ik\ell_2} \end{pmatrix}$$

$$= \frac{1}{2n} \begin{pmatrix} (1+n^2)\, e^{-ik(\ell_1+\ell_2)} & (1-n^2)\, e^{ik(\ell_2-\ell_1)} \\ (1-n^2)\, e^{ik(\ell_1-\ell_2)} & (1+n^2)\, e^{ik(\ell_1+\ell_2)} \end{pmatrix} . \quad (A3.3)$$

The scattering matrix $\overline{S}$ is then given by

$$\overline{S} = \frac{1}{r_{22}} \begin{pmatrix} r_{12} & 1 \\ 1 & -r_{21} \end{pmatrix}$$

$$= \frac{1}{1+n^2} \begin{pmatrix} (1-n^2)\, e^{-i2k\ell_1} & 2ne^{-ik(\ell_1+\ell_2)} \\ 2ne^{-ik(\ell_1+\ell_2)} & (n^2-1)\, e^{-i2k\ell_2} \end{pmatrix} . \quad (A3.4)$$

Comparing eq (A3.2a,b) with eq (A3.4), we obtain the following values for ℓ_1, ℓ_2, and n for equivalency:

$$-2k\ell_1 = \psi_{11} + (2N-1)\pi \quad (A3.5a)$$

$$-2k\ell_2 = \psi_{22} + 2M\pi \qquad \text{(A3.5b)}$$

$$n^2 = (1 + |S_{11}|)/(1 - |S_{11}|) \qquad \text{(A3.5c)}$$

where M and N are arbitrary integers subject to the constraint, $2(M + N) - 1 = N_o$, which is imposed by eq (A3.2b).

APPENDIX IV

EXPRESSIONS FOR THE COMPLEX FIELD AMPLITUDES a AND b AT THE TWO PORTS OF A TEM CELL DUE TO A DIPOLE RADIATOR INSIDE THE CELL

In this appendix we consider a TEM cell with mismatched transitions which may be represented by the equivalent circuit shown in figure 9, where the equivalent circuits of the individual transitions are enclosed by dotted rectangles. Each of the transitions is represented by two sections of transmission lines coupled by an ideal transformer. As shown in Appendix III, any arbitrary, lossless, reciprocal two-port junction can be represented by such an equivalent circuit. In figure 9 the complex amplitudes a and b, as given by eq (2.10a), depend upon the strength and the nature of the dipole radiating system and are real if the radiator consists of a single electric dipole. The complex amplitudes of the incident and reflected fields at the input ends of the transformers are indicated by a_1, b_1, a_1', and b_1', as shown. Noting that the scattering matrix of an ideal transformer, with an input to output turns ratio of 1:n, is given by

$$\overline{S} = \frac{1}{1 + n^2} \begin{pmatrix} 1 - n^2 & 2n \\ 2n & -(1 - n^2) \end{pmatrix} , \qquad \text{(A4.1)}$$

we obtain the following relations among $\tilde{a}$, $\tilde{b}$, a_1, and b_1:

$$\begin{pmatrix} \tilde{a} \\ \tilde{b} \end{pmatrix} = S_{12_{\substack{a \\ b}}} \exp(-ik\ell_{2_{\substack{a \\ b}}}) \begin{pmatrix} a_1 \\ b_1 \end{pmatrix} , \qquad \text{(A4.2a)}$$

where

$$S_{12_{\substack{a \\ b}}} = 2n_{\substack{a \\ b}} / (n^2_{\substack{a \\ b}} + 1) , \qquad \text{(A4.2b)}$$

and we made use of the fact that the output ports of the cell are terminated by matched loads. Noting further that

$$\begin{pmatrix} a'_1 \\ b'_1 \end{pmatrix} = S_{11\substack{a \\ b}} \begin{pmatrix} a_1 \\ b_1 \end{pmatrix} , \tag{A4.3}$$

we can write the following equations for a_1 and b_1 in terms of a and b by physical inspection,

$$a_1 = a\, e^{-ik(\ell'_{1a}-z)} + S_{11b} b_1 e^{-ik(\ell'_{1a}+\ell'_{1b})} , \tag{A4.4a}$$

$$b_1 = b\, e^{-ik(\ell'_{1b}+z)} + S_{11a} a_1 e^{-ik(\ell'_{1a}+\ell'_{1b})} , \tag{A4.4b}$$

where

$$S_{11\substack{a \\ b}} = (1 - n_{\substack{a \\ b}}^2)/(1 + n_{\substack{a \\ b}}^2) , \tag{A4.4c}$$

and

$$\ell'_{1\substack{a \\ b}} = \ell_{1\substack{a \\ b}} + \tfrac{1}{2} L . \tag{A4.4d}$$

Eliminating a_1 and b_1 from eqs (A4.4a) and (A4.4b) with the aid of eq (A4.2a), we can write a and b in terms of $\tilde{a}$ and $\tilde{b}$ as

$$\begin{pmatrix} a \\ b \end{pmatrix} = \begin{Bmatrix} \frac{1}{S_{12a}} e^{ik(\ell'_{1a}+\ell_{2a}-z)} & -\frac{S_{11b}}{S_{12b}} e^{-ik(\ell'_{1b}-\ell_{2b}+z)} \\ -\frac{S_{11a}}{S_{12a}} e^{-ik(\ell'_{1a}-\ell_{2a}-z)} & \frac{1}{S_{12b}} e^{ik(\ell'_{1b}+\ell_{2b}+z)} \end{Bmatrix} \begin{pmatrix} \tilde{a} \\ \tilde{b} \end{pmatrix} \tag{A4.5a}$$

which upon inversion gives

$$\begin{pmatrix} \tilde{a} \\ \tilde{b} \end{pmatrix} = \frac{1}{\Delta} \begin{bmatrix} \frac{1}{S_{12b}} e^{ik(\ell'_{1b}+\ell_{2b}+z)} & \frac{S_{11b}}{S_{12b}} e^{-ik(\ell'_{1b}-\ell_{2b}+z)} \\ \frac{S_{11a}}{S_{12a}} e^{-ik(\ell'_{1a}-\ell_{2a}-z)} & \frac{1}{S_{12a}} e^{ik(\ell'_{1a}+\ell_{2a}-z)} \end{bmatrix} \begin{pmatrix} a \\ b \end{pmatrix} , \tag{A4.5b}$$

where

$$\Delta = \frac{1}{S_{12a}S_{12b}} \{ e^{ik(\ell'_{1a}+\ell'_{1b}+\ell_{2a}+\ell_{2b})} - S_{11a}S_{11b} e^{ik(\ell_{2a}+\ell_{2b}-\ell'_{1a}-\ell'_{1b})} \} . \tag{A4.5c}$$

For the case of an electric dipole radiator, a and b are equal and the ratio of the complex amplitudes at the positive port with the radiator at z = +g and z = -g is given from eq (A4.5b) as

$$\tilde{a}_r = \frac{\tilde{a}(z=+g)}{\tilde{a}(z=-g)} = \frac{e^{ik(\ell'_{1b}+g)} + S_{11b} e^{-ik(\ell'_{1b}+g)}}{e^{ik(\ell'_{1b}-g)} + S_{11b} e^{-ik(\ell'_{1b}-g)}}$$

$$= \frac{e^{i2kg} + S_{11b} e^{-i2k\ell'_{1b}}}{e^{-i2kg} + S_{11b} e^{-i2k\ell'_{1b}}} e^{-i2kg} . \tag{A4.6}$$

Using this relation, we can write

$$\frac{\tilde{a}_r e^{i2kg} + 1}{\tilde{a}_r e^{i2kg} - 1} = [\cos(2kg) + S_{11b} e^{-i2k\ell'_{1b}}]/i \sin(2kg) ,$$

and using eqs (A4.4c) and (A4.4d), we can obtain the solution for n_b and ℓ_{1b} in the following form:

$$\frac{1 - n_b^2}{1 + n_b^2} e^{-i2k\ell_{1b}} = \{i(\frac{\tilde{a}_r e^{i2kg} + 1}{\tilde{a}_r e^{i2kg} - 1}) \sin(2kg) - \cos(2kg)\} e^{ikL} . \tag{A4.7}$$

In a similar manner, we start with the ratio $\tilde{b}_r = \tilde{b}(-g)/\tilde{b}(+g)$ and obtain

$$\frac{1 - n_a^2}{1 + n_a^2} e^{-i2k\ell_{1a}} = \{i(\frac{\tilde{b}_r e^{i2kg} + 1}{\tilde{b}_r e^{i2kg} - 1}) \sin(2kg) - \cos(2kg)\} e^{ikL} . \tag{A4.8}$$

APPENDIX V.

THE RELATION BETWEEN THE CASCADING PARAMETERS OF A TEM CELL AND THE EQUIVALENT CIRCUIT PARAMETERS, ℓ_{2a} and ℓ_{2b}, OF THE INDIVIDUAL TRANSITIONS

A TEM cell with mismatched transitions may be represented by the equivalent circuit shown in figure 9, which is essentially made of two dissimilar networks, of the type shown in figure 8, cascaded in reverse order. Hence, the cascading matrix of the entire cell is given by [see eq (A3.3)]:

$$\bar{R} = \bar{R}_b \, \bar{R}_a \tag{A5.1a}$$

where

$$\bar{R}_b = \frac{1}{2n_b} \begin{Bmatrix} (1+n_b^2)\, e^{-ik(\ell'_{1b}+\ell_{2b})} & -(1-n_b^2)\, e^{ik(\ell'_{1b}-\ell_{2b})} \\ -(1-n_b^2)\, e^{ik(\ell_{2b}-\ell'_{1b})} & (1+n_b^2)\, e^{ik(\ell'_{1b}+\ell_{2b})} \end{Bmatrix}, \tag{A5.1b}$$

and

$$\bar{R}_a = \frac{1}{2n_a} \begin{Bmatrix} (1+n_a^2)\, e^{-ik(\ell'_{1a}+\ell_{2a})} & (1-n_a^2)\, e^{ik(\ell_{2a}-\ell'_{1a})} \\ (1-n_a^2)\, e^{ik(\ell'_{1a}-\ell_{2a})} & (1+n_a^2)\, e^{ik(\ell'_{1a}+\ell_{2a})} \end{Bmatrix}. \tag{A5.1c}$$

We note that $\bar{R}_b$ is <u>not</u> obtained from $\bar{R}_a$ by simple interchange of the subscripts a and b. This is because of the reverse order in which the parameters ℓ'_{1b}, ℓ_{2b}, and n_b present themselves in the equivalent circuit as opposed to the parameters ℓ'_{1a}, ℓ_{2a}, and n_a. Taking the product $\bar{R} = \bar{R}_b \, \bar{R}_a$, we obtain

$$R_{11} = \frac{1}{4n_a n_b}\left[(1+n_a^2)(1+n_b^2)\exp\{-ik(L'+\ell_{2s})\}\right.$$
$$\left.-(1-n_a^2)(1-n_b^2)\exp\{ik(L'-\ell_{2s})\}\right] , \qquad \text{(A5.2a)}$$

$$R_{22} = \frac{1}{4n_a n_b}\left[(1+n_a^2)(1+n_b^2)\exp\{ik(L'+\ell_{2s})\}\right.$$
$$\left.-(1-n_a^2)(1-n_b^2)\exp\{-ik(L'-\ell_{2s})\}\right] , \qquad \text{(A5.2b)}$$

and

$$R_{12} = R_{21}^* = \frac{1}{4n_a n_b}\left[(1-n_a^2)(1+n_b^2)\exp\{-ik(L'-\ell_{2d})\}\right.$$
$$\left.-(1+n_a^2)(1-n_b^2)\exp\{ik(L'+\ell_{2d})\}\right] , \qquad \text{(A5.2c)}$$

where

$$L' = \ell_{1a} + \ell_{1b} + L , \qquad \text{(A5.2d)}$$

$$\ell_{2d} = \ell_{2a} - \ell_{2b} , \qquad \text{(A5.2e)}$$

$$\ell_{2s} = \ell_{2a} + \ell_{2b} . \qquad \text{(A5.2f)}$$

Denoting

$$U_{11} = 2n_a n_b R_e(R_{11}) = n_a n_b(R_{11} + R_{22}) \qquad \text{(A5.3a)}$$

$$V_{11} = 2n_a n_b I_m(R_{11}) = n_a n_b(R_{11} - R_{22}) / i \qquad \text{(A5.3b)}$$

$$U_{12} = 2n_a n_b R_e(R_{12}) = n_a n_b(R_{12} + R_{21}) \qquad \text{(A5.3c)}$$

$$V_{12} = 2n_a n_b I_m(R_{12}) = n_a n_b(R_{12} - R_{21}) / i , \qquad \text{(A5.3d)}$$

we can establish the following matrix equations in a straightforward manner:

$$\begin{bmatrix} -(1+n_a^2 n_b^2)\sin kL' & (n_a^2+n_b^2)\cos kL' \\ -(n_a^2+n_b^2)\cos kL' & -(1+n_a^2 n_b^2)\sin kL' \end{bmatrix} \begin{bmatrix} \sin(k\ell_{2s}) \\ \cos(k\ell_{2s}) \end{bmatrix} = \begin{bmatrix} U_{11} \\ V_{11} \end{bmatrix}, \tag{A5.4}$$

$$\begin{bmatrix} (1-n_a^2 n_b^2)\sin(kL') & -(n_a^2-n_b^2)\cos(kL') \\ -(n_a^2-n_b^2)\cos(kL') & -(1-n_a^2 n_b^2)\sin(kL') \end{bmatrix} \begin{bmatrix} \sin(k\ell_{2d}) \\ \cos(k\ell_{2d}) \end{bmatrix} = \begin{bmatrix} U_{12} \\ V_{12} \end{bmatrix} \tag{A5.5}$$

which have the solution:

$$\begin{bmatrix} \sin(k\ell_{2s}) \\ \cos(k\ell_{2s}) \end{bmatrix} = \frac{1}{\Delta_s} \begin{bmatrix} -(1+n_a^2 n_b^2)\sin(kL') & -(n_a^2+n_b^2)\cos(kL') \\ (n_a^2+n_b^2)\cos(kL') & -(1+n_a^2 n_b^2)\sin(kL') \end{bmatrix} \begin{bmatrix} U_{11} \\ V_{11} \end{bmatrix}, \tag{A5.6a}$$

$$\begin{bmatrix} \sin(k\ell_{2d}) \\ \cos(k\ell_{2d}) \end{bmatrix} = \frac{1}{\Delta_d} \begin{bmatrix} -(1-n_a^2 n_b^2)\sin(kL') & (n_a^2-n_b^2)\cos(kL') \\ (n_a^2-n_b^2)\cos(kL') & (1-n_a^2 n_b^2)\sin(kL') \end{bmatrix} \begin{bmatrix} U_{12} \\ V_{12} \end{bmatrix}, \tag{A5.6b}$$

where

$$\Delta_s = (n_a^2+n_b^2)^2 \cos^2 kL' + (1+n_a^2 n_b^2)^2 \sin^2 kL' , \tag{A5.6c}$$

$$\Delta_d = -(1- n_a^2 n_b^2)^2 \sin^2 kL' - (n_a^2 - n_b^2) \cos^2 kL' \ . \qquad \text{(A5.6d)}$$

The above eqs (A5.6a) to (A5.6d) uniquely determine the values of ℓ_{2s} and ℓ_{2d}, which in turn will give the parameters ℓ_{2a} and ℓ_{2b}.

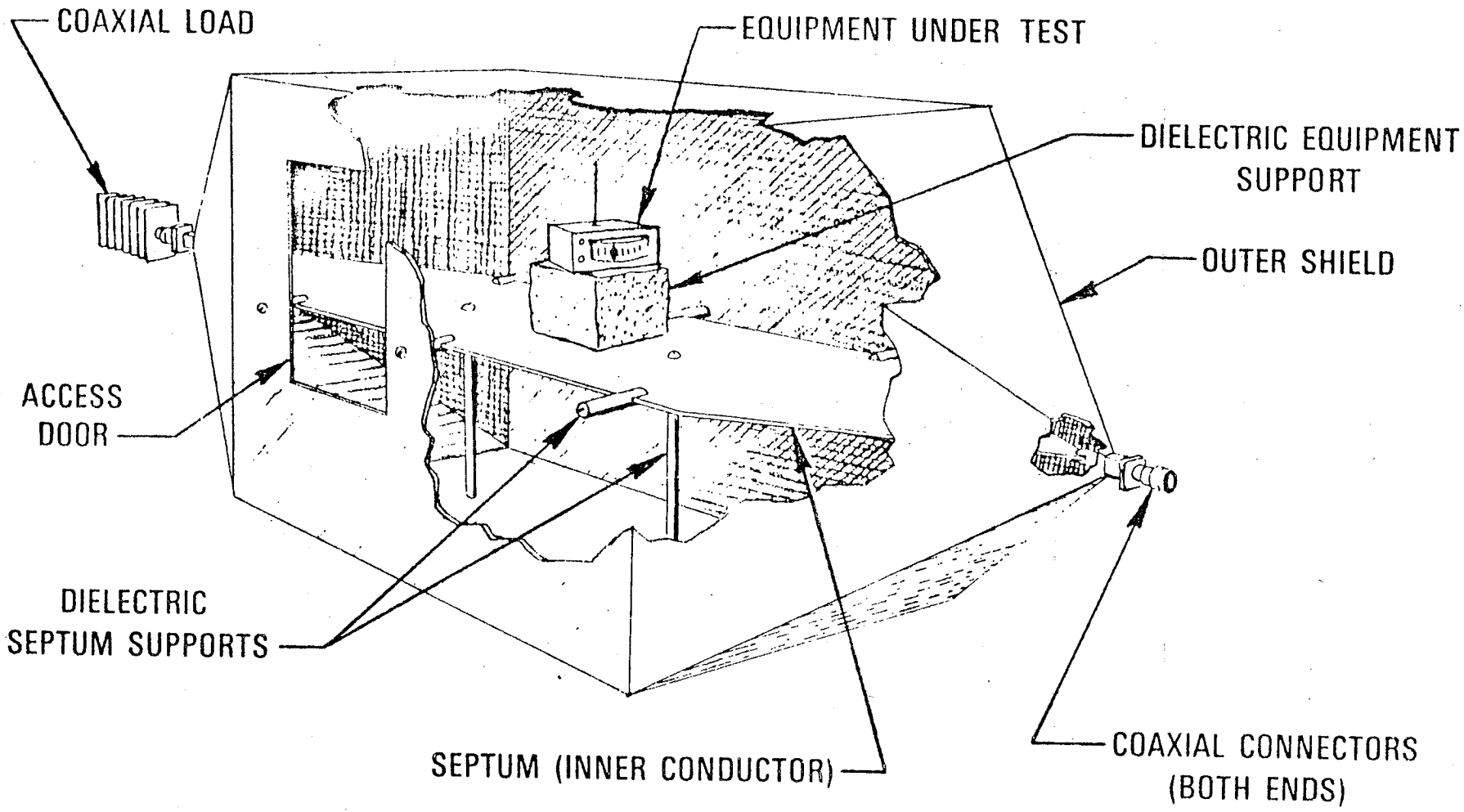

Figure 1. Diagram of an NBS TEM cell.

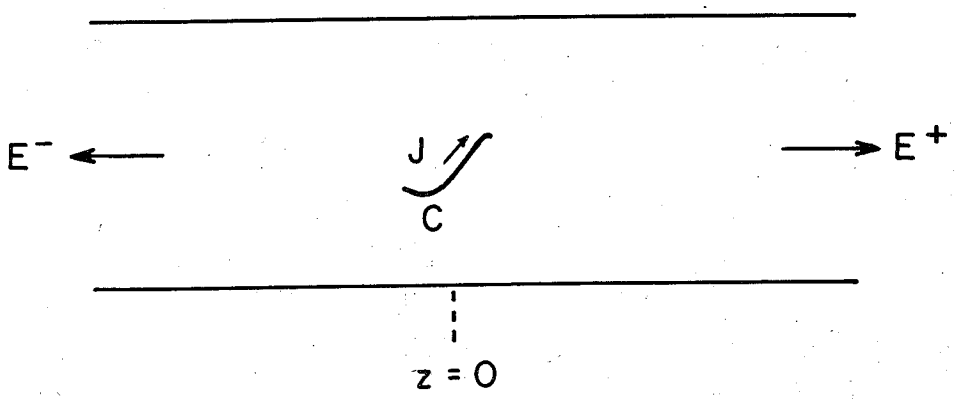

Figure 2. An arbitrary current filament in a uniform cylindrical guide

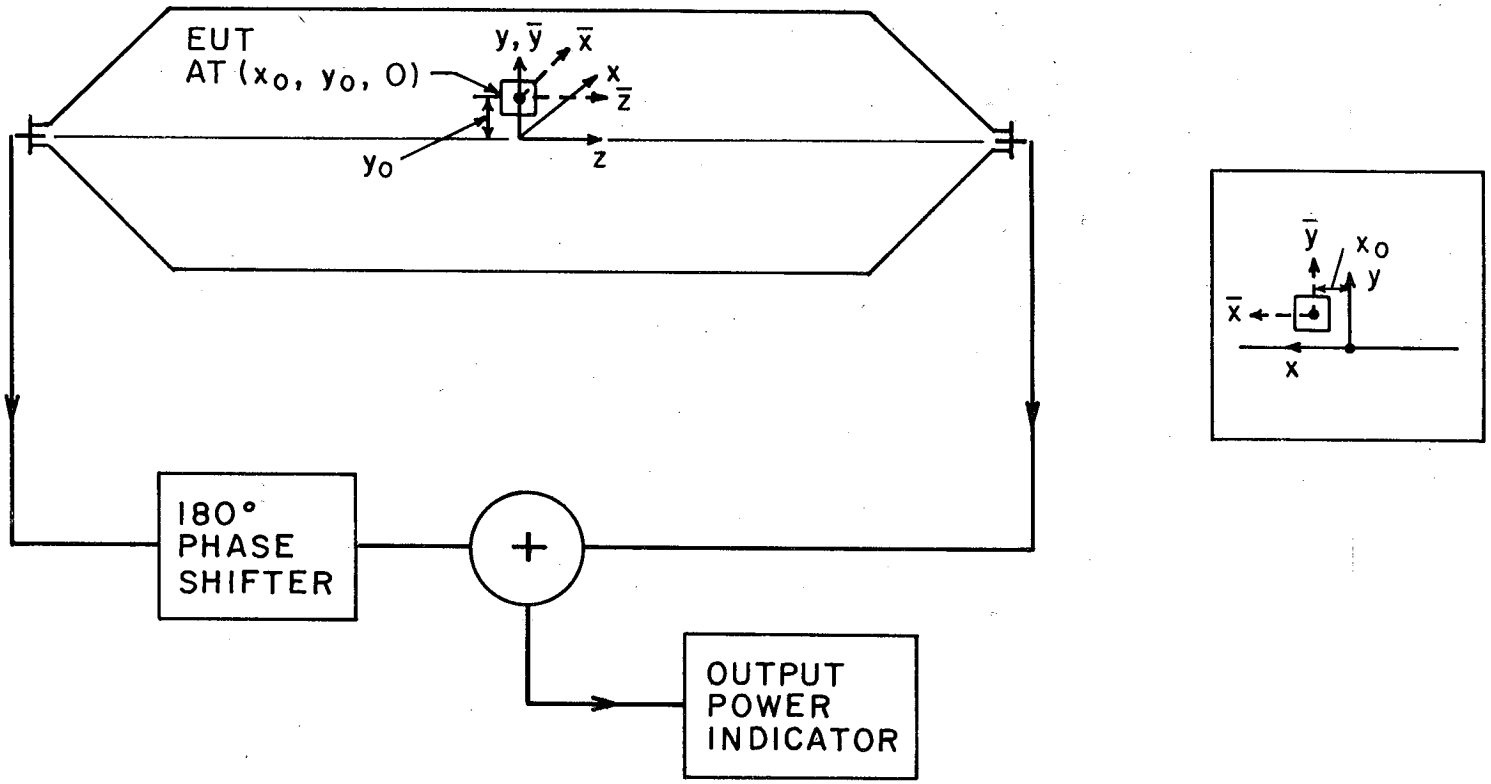

Figure 3. Test setup for determining radiation characteristics of small electric and/or magnetic dipole sources.

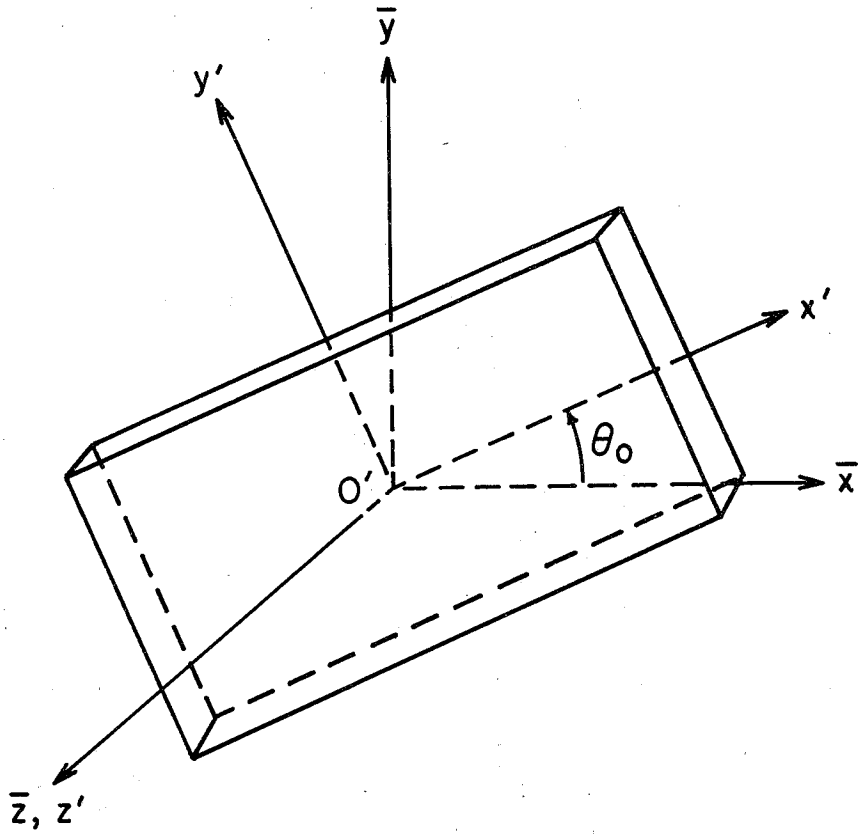

Figure 4a. One orientation of the equipment under test (EUT) with respect to x-, y-, z-axes of the cell.

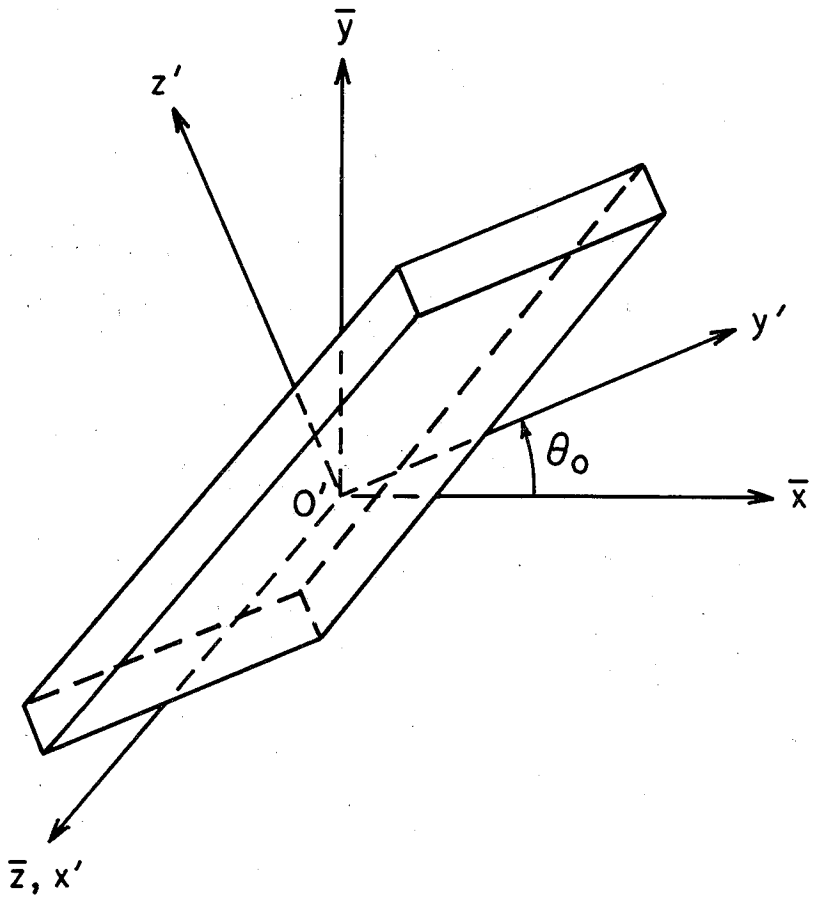

Figure 4b. Another orientation of the EUT with respect to the cell axes.

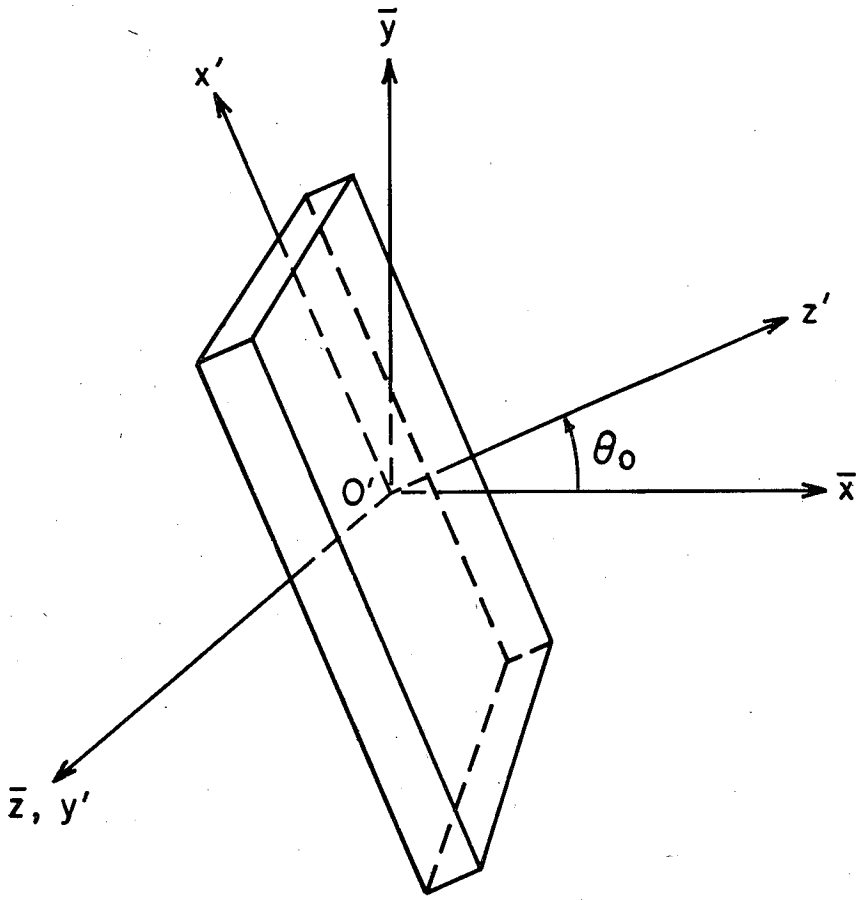

Figure 4c. A third orientation of the EUT with respect to the cell axes.

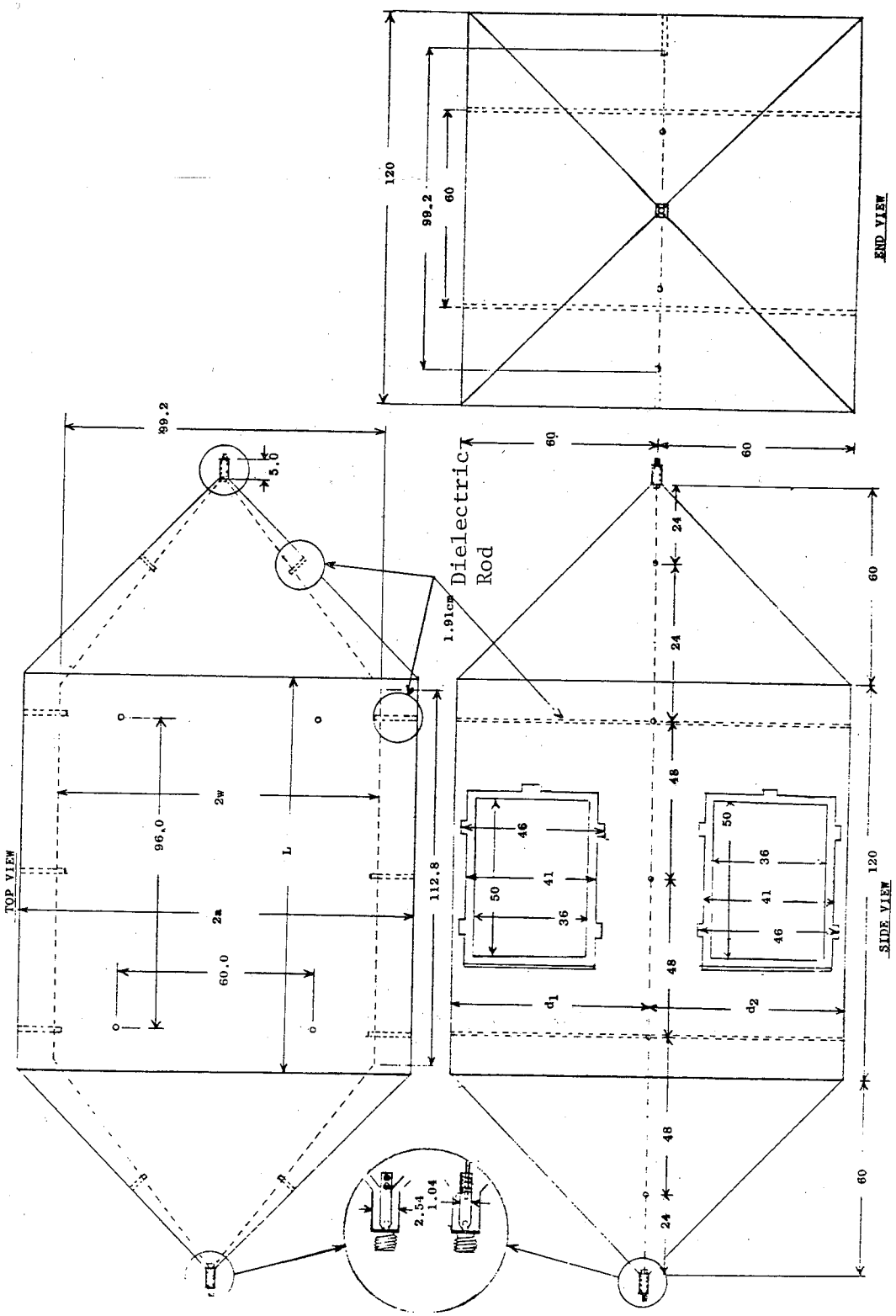

Figure 5. Cross-sectional views of a 1.20 x 1.20 x 2.40 m^3 symmetric rectangular coaxial TEM cell developed at NBS.

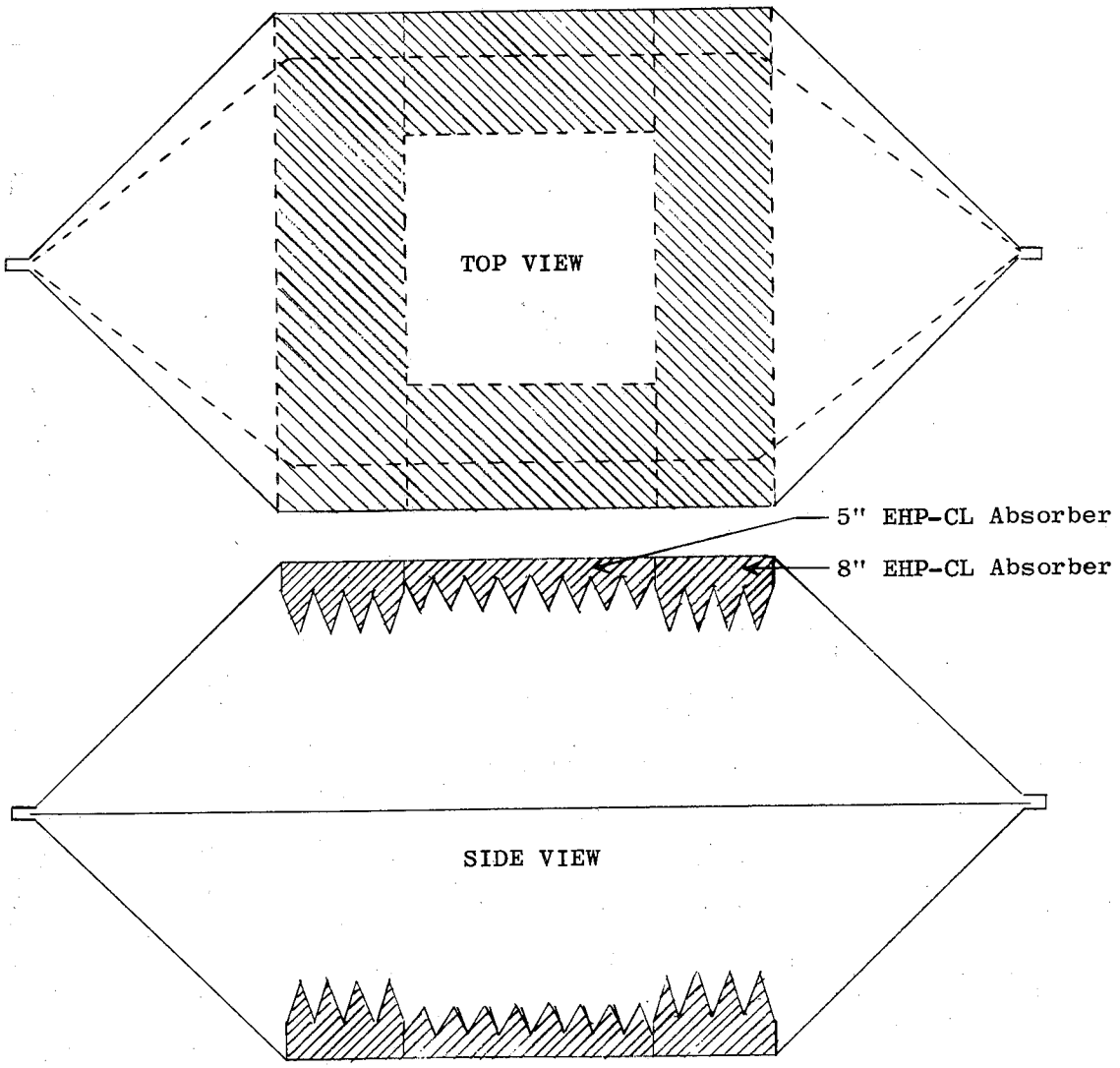

Figure 6. Absorber loading in the TEM cell shown in figure 5.

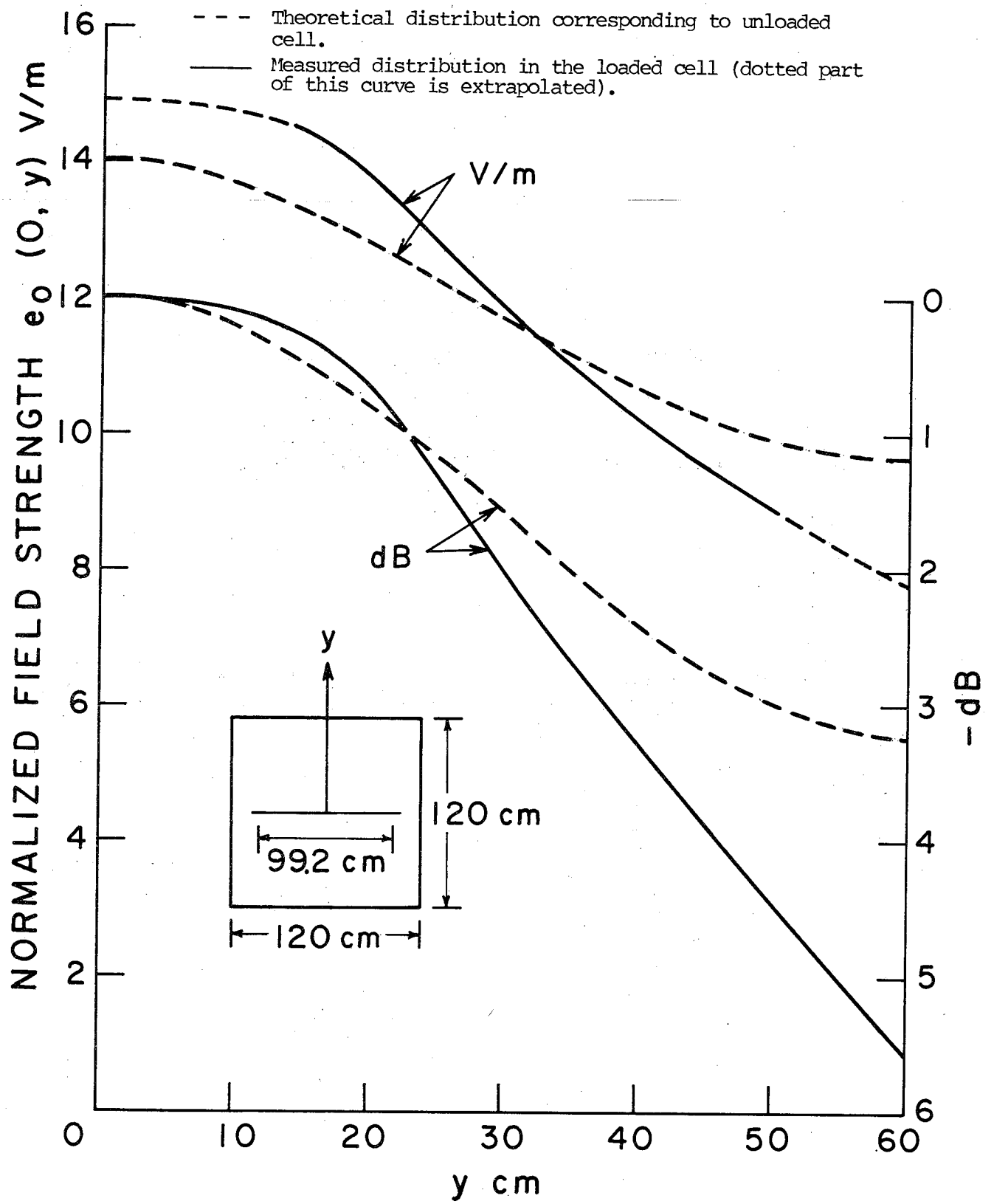

Figure 7. Normalized field strength distribution in the TEM cell shown in figure 5.

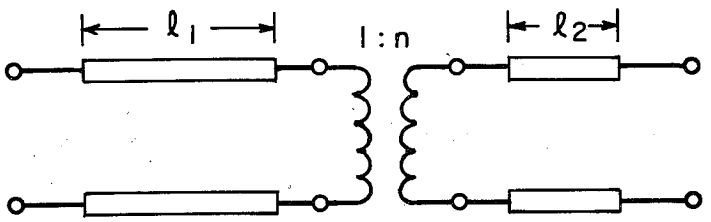

Figure 8. Scattering matrix representation of a cell with mismatched transitions.

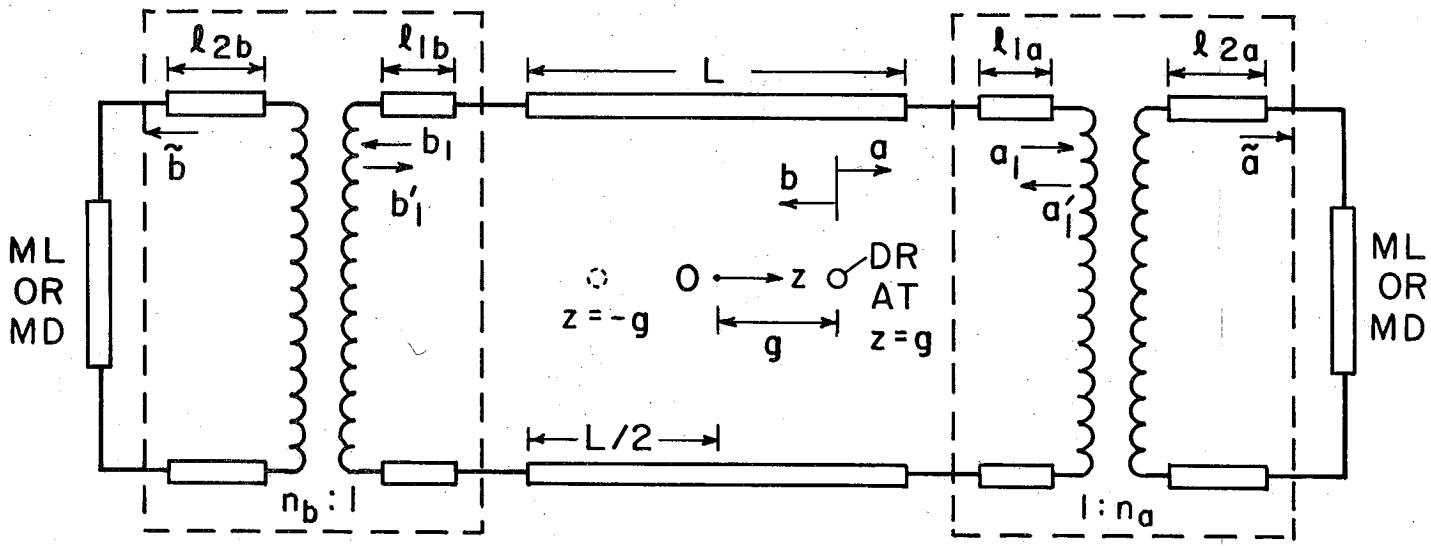

ML: MATCHED LOAD; MD: MATCHED DETECTOR;
DR: DIPOLE RADIATOR

Figure 9. Equivalent circuit representation of a TEM cell with mismatched transitions.

NBS-114A (REV. 9-78)

U.S. DEPT. OF COMM. BIBLIOGRAPHIC DATA SHEET	1. PUBLICATION OR REPORT NO. NBS TN-1017	2. Gov't. Accession No.	3. Recipient's Accession No.

4. TITLE AND SUBTITLE

Characterization of Electrically Small Radiating Sources by Tests Inside a Transmission Line Cell

5. Publication Date February 1980

6. Performing Organization Code

7. AUTHOR(S)

Ippalapalli Sreenivasiah, David C. Chang, and Mark T. Ma

8. Performing Organ. Report No.

9. PERFORMING ORGANIZATION NAME AND ADDRESS

NATIONAL BUREAU OF STANDARDS
DEPARTMENT OF COMMERCE
WASHINGTON, DC 20234

10. Project/Task/Work Unit No.

11. Contract/Grant No.

12. SPONSORING ORGANIZATION NAME AND COMPLETE ADDRESS *(Street, City, State, ZIP)*

Same as Item 9.

13. Type of Report & Period Covered

14. Sponsoring Agency Code

15. SUPPLEMENTARY NOTES

☐ Document describes a computer program; SF-185, FIPS Software Summary, is attached.

16. ABSTRACT *(A 200-word or less factual summary of most significant information. If document includes a significant bibliography or literature survey, mention it here.)*

An electrically small radiating source of arbitrary nature may be modeled by an equivalent dipole system consisting of three orthogonal electric dipoles and three orthogonal magnetic dipoles, each excited with arbitrary phase. An experimental procedure for determining the emission characteristics of such an equivalent dipole system by tests inside a single-mode transmission line cell is described in this report, followed by some experimental results.

17. KEY WORDS *(six to twelve entries; alphabetical order; capitalize only the first letter of the first key word unless a proper name; separated by semicolons)*

Electrical dipole; electrically small radiators, magnetic dipole, TEM cell.

18. AVAILABILITY ☒ Unlimited

☐ For Official Distribution. Do Not Release to NTIS

☒ Order From Sup. of Doc., U.S. Government Printing Office, Washington, DC 20402, SD Stock No. SN003-003-02157-1

☐ Order From National Technical Information Service (NTIS), Springfield, VA. 22161

19. SECURITY CLASS (THIS REPORT) UNCLASSIFIED

21. NO. OF PRINTED PAGES 67

20. SECURITY CLASS (THIS PAGE) UNCLASSIFIED

22. Price $3.50

☆U.S. GOVERNMENT PRINTING OFFICE: 1980-0-677-096/1231 USCOMM-DC